Low-Level Radioactive-Waste Burial at the Palos Forest Preserve, Illinois: Geology and Hydrology of the Glacial Drift, as Related to the Migration of Tritium

By JULIO C. OLIMPIO

U.S. GEOLOGICAL SURVEY WATER-SUPPLY PAPER 2226

UNITED STATES DEPARTMENT OF THE INTERIOR
WILLIAM P. CLARK, Secretary

GEOLOGICAL SURVEY
Dallas L. Peck, Director

UNITED STATES GOVERNMENT PRINTING OFFICE: 1984

For sale by the Superintendent of Documents
U.S. Government Printing Office
Washington, D.C. 20402

Library of Congress Cataloging in Publication Data

Olimpio, Julio C.
Low-level radioactive-waste burial at the Palos Forest Preserve, Illinois.

(Geological Survey water-supply paper; 2226)
Bibliography: p.
Supt. of Docs. no.: I 19.13:2226
1. Radioactive waste disposal in the ground—Illinois—Palos Forest Preserve. 2. Water, Underground—Pollution—Illinois—Palos Forest Preserve. 3. Radioisotopes—Migration. 4. Tritium. I. Title. II. Series.
TD898.044 1983 621.48'38 82-600382

CONTENTS

Abstract 1
Introduction 1
Problems and objectives 2
General method of investigation 3
Acknowledgments 3
Description of the Plot M site 3
    Location and geographic setting 3
    History 3
Drilling and subsurface exploration program 7
Regional geology 8
Drift at Plot M 8
    Geology 8
        Lithology and mineralogy 9
        Lithostratigraphy 13
    Hydrogeology 17
        Sources of water 17
            Precipitation 17
            Evapotranspiration 21
            Local runoff 21
            Ground-water flow 21
        Ground water 21
            The unsaturated zone 21
            The saturated zone 21
            Hydraulic conductivity 26
            Total head and ground-water flow 26
Ground water in the Silurian dolomite 28
Tritium migration 28
    Studies at Plot M 28
    The tritium plume at Plot M 28
        Section *E–E′* 28
        Section *B–B′* 28
        Section *A–A′* 28
Discussion 32
    The single slug theory 32
    Tritium migration rate 32
    Factors favoring tritium migration at the Plot M site 32
    Factors limiting tritium migration at the Plot M site 33
Summary and conclusions 33
Selected references 34

FIGURES

1. Map showing location of Plot M in the Palos Forest Preserve, Cook County, Ill. 2
2. Map of the Plot M burial site showing topography, intermittent streams, test well locations, and lines of cross-sections *A–A′* through *E–E′* 4
3. Graph showing the tritium content of water from the Red Gate Woods well (forest preserve well 5167) and from the well (forest preserve well 5159) opposite the Red Gate Woods well next to the Illinois and Michigan Canal 5
4. Graph showing the comparison of three different geophysical logs to lithology in test well 28 9

5. Cross section showing correlation of natural-gamma logs from test wells 4, 5, and 11 **14**
6. Geologic section *E–E′* of the Plot M site **15**
7. Geologic section *D–D′* of the Plot M site **16**
8. Geologic section *C–C′* of the Plot M site **17**
9. Geologic section *B–B′* of the Plot M site **18**
10. Geologic section *A–A′* of the Plot M site **19**
11. Hydrographs showing monthly variation in precipitation and water levels in test wells at the Plot M site, August 1976 to April 1980 **20**
12. Cross-section *E–E′* through the Plot M site showing the vertical hydraulic head distribution and principal ground-water flow direction—May 1980 **27**
13. Cross-section *E–E′* through the Plot M site showing the extent of tritium migration and levels of concentration in soil moisture collected from core samples of the drift **29**
14. Cross-section *B–B′* on the north side of the Plot M site showing the extent of tritium migration and levels of concentration in soil moisture collected from core samples of the drift **30**
15. Cross-section *A–A′* 50 meters north of the Plot M site showing the extent of tritium migration and levels of concentration in the drift in soil moisture collected from core samples of the drift **31**

TABLES

1. Test-well construction data and lithologic description of cores of test well 26 at Plot M **6**
2. Site and well-construction data of bedrock wells in the forest preserve near Plot M **8**
3. Geologic time-stratigraphic classification, rock-stratigraphic classification, and general description of the drift at the Plot M site **10**
4. Grain-size and composition data from samples of glacial drift at Plot M **11**
5. Hydraulic conductivity of glacial drift at Plot M **22**
6. Total porosity, bulk density, specific gravity, and surface-area data of samples of glacial drift at Plot M **25**

Low-Level Radioactive-Waste Burial at the Palos Forest Preserve, Illinois: Geology and Hydrology of the Glacial Drift, as Related to the Migration of Tritium

By Julio C. Olimpio

Abstract

A low-level radioactive-waste burial site is located in Palos Forest Preserve, about 22 kilometers southwest of Chicago, Illinois. Between 1943 and 1949 the site, named Plot M, was filled with radioactive waste from the first Argonne National Laboratory and from the University of Chicago Metallurgical Laboratory. Since 1973, tritium concentration levels up to 14 nanocuries per liter have been measured in water samples collected from a well 360 meters from the burial site.

The U.S. Geological Survey is studying the geologic, hydrologic, and geochemical properties of the glacial drift and underlying bedrock at the Plot M site to determine the factors that control the movement of radionuclides. Test wells were drilled into the drift to collect water and core samples for laboratory analysis, to gather geologic and hydrologic data, and to conduct geophysical surveys.

Plot M is located in drift that ranges in thickness from 25 to 45 meters. The drift is a stratified sequence of clay- and silt-rich sediments that contain thin, interstratified sand layers. The silt content of the drift increases with depth. The permeability of the drift, as indicated by field and laboratory hydraulic conductivity tests, ranges from 1.0×10^{-6} to 1.0×10^{-8} centimeters per second.

A tritium plume, the contaminated zone in the drift in which tritium concentration levels exceed 10 nanocuries per liter of water, extends horizontally northward from Plot M at least 50 meters and vertically downward to bedrock. The center of the plume, where tritium concentration levels are as high as 50,000 nanocuries per liter, is approximately 15 meters beneath the burial site. The size, shape, and "bull's-eye" concentration pattern indicate that the plume is a single slug and that the site no longer releases tritium into the drift. The leading edge, or front, of the plume (the 10 nanocuries per liter boundary) left the burial site in either the late 1940's or the early 1950's and intersected the underlying bedrock surface before 1973. The calculated movement rate of the front is 6.3×10^{-6} centimeters per second.

Several key factors that control both the concentration level and the extent of migration of tritium in the drift at Plot M are

1. The limited amount of tritiated waste buried at Plot M.
2. The long period of time that has elapsed since the waste was buried (30–35 years) relative to the radioactive half-life of tritium (12.3 years).
3. The great thickness and low permeability of the glacial drift at the site.

INTRODUCTION

In early 1943, the U.S. Army Corps of Engineers leased land from the Cook County Forest Preserve District to build a radioisotope research facility. The facility formed part of the Metallurgical Laboratory operated by the University of Chicago for the Manhattan Engineer District (the Manhattan Project). The facility, known as Site A, housed three of the world's first nuclear reactors. Plot M was the burial site for the low-level radioactive waste derived from Metallurgical Laboratory operations (fig. 1).

From 1943 to 1948, radioactive waste delivered to Plot M was placed in simple 2.5-m-deep trenches. Soil was used to cover the waste and to reduce the level of radiation. During 1948–49, waste was put in steel bins, which, in turn, were placed in trenches and covered with soil. In June 1949, the bins were removed and burial operations were discontinued. Work at Plot M ended in 1956 with the construction of an inverted concrete box that covered the entire burial site.

The Argonne National Laboratory (ANL) has conducted a radiological monitoring program at Plot M since 1948. In 1954, at the request of ANL, the U.S. Geological Survey studied the geologic, hydrologic, and chemical characteristics of the glacial drift at Plot M (W. J. Drescher, written commun., 1954) and advised ANL on its environmental monitoring program. In 1973, tritium was detected in water from a dolomite bedrock well at the Red Gate Woods picnic area, and the ANL monitoring program was expanded to include the Red Gate Woods well and other nearby forest preserve wells.

The study of ground-water flow and tritium migration at Plot M described in this paper began in 1978. Re-

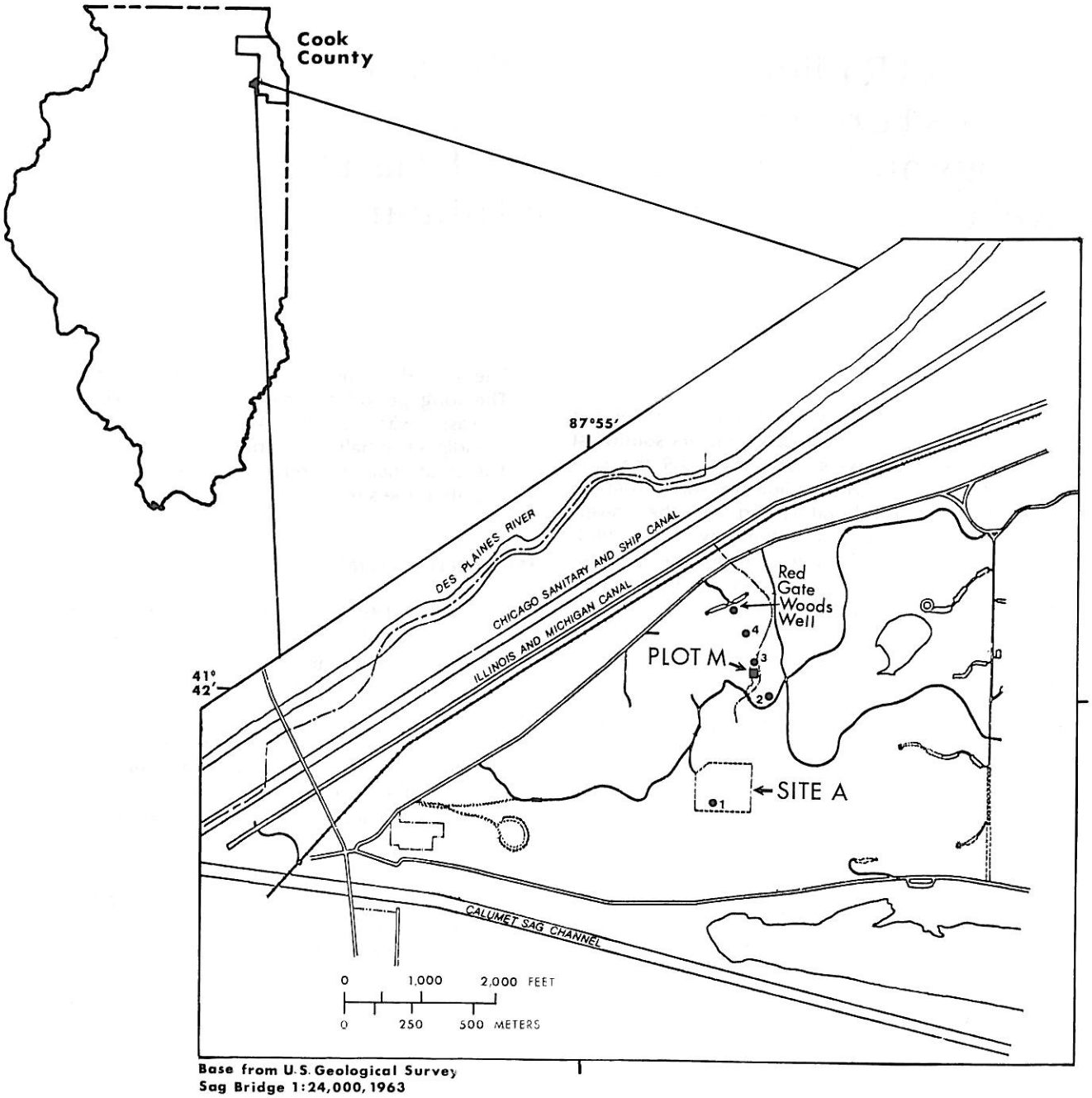

Figure 1. Location of Plot M in the Palos Forest Preserve, Cook County, Ill.

sults of the study described below represent data gathered and conclusions drawn after 2 years of investigation.

PROBLEMS AND OBJECTIVES

The study attempts to answer several questions that arose after the discovery of tritium in the water at the Red Gate Woods well. Assuming that Plot M is the source, how does tritium migrate from Plot M to the Red Gate Woods well? Does it move with ground water along pathways entirely within the glacial drift, or along pathways through both the drift and the underlying bedrock? What is the rate and extent of tritium migration in the drift and the bedrock? Do surface and subsurface conditions at the site encourage migration? Are there conditions that work to retard migration? Frequent use of the land and water in the forest preserve at Plot M year-around emphasizes the need for answers to these questions.

The main objectives of this study are to determine the geologic, hydrologic, and geochemical properties of the drift that control the migration of tritium from the burial site to the underlying bedrock and to determine the present extent of tritium in the drift. A third objective is to determine the rate and direction of tritium movement in water in the bedrock. The results of the study are needed by the U.S. Department of Energy to evaluate the need for remedial action at the Plot M site.

GENERAL METHOD OF INVESTIGATION

The method of investigation was based initially on the following information:

1. The results of preliminary numerical ground-water flow models.
2. Simplified assumptions concerning the movement of ground water and tritium in drift and in dolomite bedrock.

Because model results showed that anisotropic geologic and hydraulic properties of the drift significantly affected ground-water flow, detailed geologic and hydrologic information from the drift was needed. Drilling at each site was accompanied by continuous split-spoon sampling of the drift to determine small-scale lithologic properties. Cores and samples were logged in the field and were sealed for laboratory analysis. In addition to field observations of the lithology, texture, color, structure, and sedimentological features exhibited by each sample, the samples also were analyzed for the following properties: mineralogy, grain-size distribution, density, porosity, hydraulic conductivity, moisture content, and tritium content.

ACKNOWLEDGMENTS

This investigation relied heavily on the Plot M environmental surveillance program conducted by the ANL. Especially helpful have been J. Sedlet, N. W. Golchert, and H. C. Svoboda of the Health Safety Section of the ANL, who have provided administrative and technical assistance throughout the project.

DESCRIPTION OF THE PLOT M SITE

Location and Geographic Setting

The Palos Forest Preserve is a wedge-shaped area in the southwestern corner of Cook County, Ill. (fig. 1). The area is hilly and lies southeast of the Illinois and Michigan Canal, the Chicago Sanitary and Ship Canal, and the Des Plaines River and north of the Calumet Sag Channel. The low-lying glacial Lake Michigan plain borders the east side of the forest preserve. In this paper, Plot M and the adjacent forest preserve land are referred to as the Plot M site.

Plot M is rectangular, about 40 m north-south by 44 m east-west (fig. 2). It is an open, grassy area on an eastward-sloping hill. The site is drained by two intermittent streams. A large stream flows through a ravine that skirts the south and east sides of the site, and a smaller stream flows in a ditch that parallels the west side of the site and swings eastward to join the large stream at a point 65 m north of Plot M. The site is approximately 215 m above sea level.

History

When the burial site was in use, a high fence topped with barbed wire prohibited animal, pedestrian, and vehicular traffic from crossing the area. A concrete wall extending 2.5 m below grade around the fenced area prevented burrowing animals from entering the site. Early records give very poor descriptions of the burial procedures used and of the identity and quantity of waste material buried. Records indicate that waste was buried in 2.5 by 2.5 by 12 m trenches; each trench, therefore, could hold roughly 75 m^3 of waste material. Eventually, 41 trenches were constructed; each was numbered and marked with a steel post and a brass tag. Spacing between the trenches ranged from 1 to 3 m. In 1956, a protective concrete cap was installed over the trenches. The cap resembles an open inverted box with vertical sides 2.6 m deep. Upon completion of the cap, the fence was removed and the entire area was covered with soil nearly 1 m thick. The corners of the site are marked; however, the individual trenches are not marked.

An ANL environmental monitoring program for Plot M was established in 1954 with the assistance of the Survey. Samples of surface water, surface soil, and augered soil core samples were collected for analyses. Samples collected through 1961 contained normal radioactivity for the Chicago area. During the period 1963–69, abnormally high alpha and beta activity was detected in surface soil samples collected 17 m northwest of the site (Golchert and Sedlet, 1978).

The first indication of subsurface movement of radionuclides was in 1973, when tritium concentration levels higher than background levels were detected in the water in the bedrock well at the Red Gate Woods picnic area. Since then the water in the well has been sampled periodically and analyzed for tritium and other radionuclides. Tritium concentration levels range from 0.25 nanocuries per liter of water (nCi/L) to 14 nCi/L (fig. 3). The pattern of fluctuating tritium concentration levels, highest during the winter and lowest during the summer, has been observed since 1973.

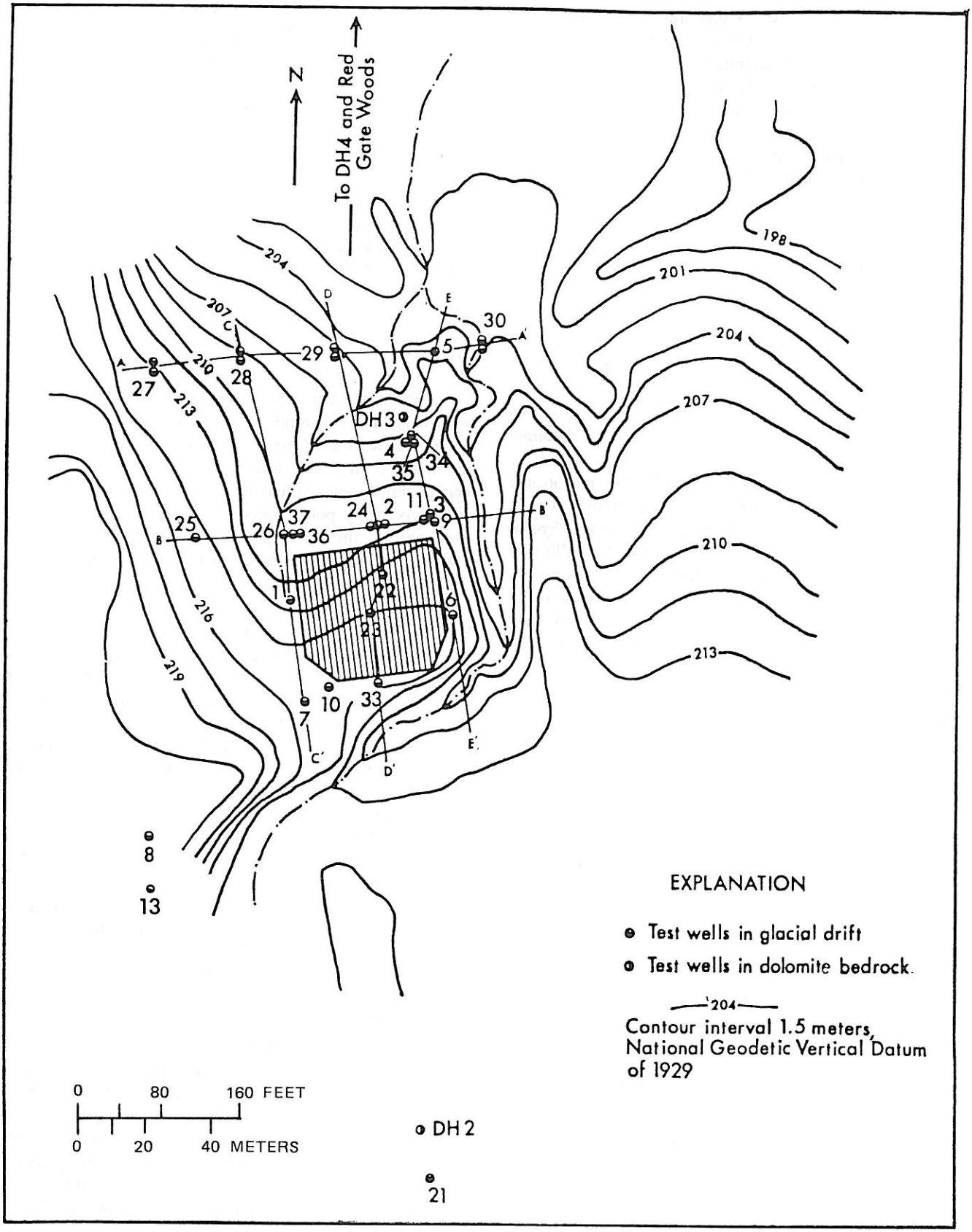

Figure 2. The Plot M burial site showing topography, intermittent streams, test well locations, and lines of cross-sections *A–A'* through *E–E'*.

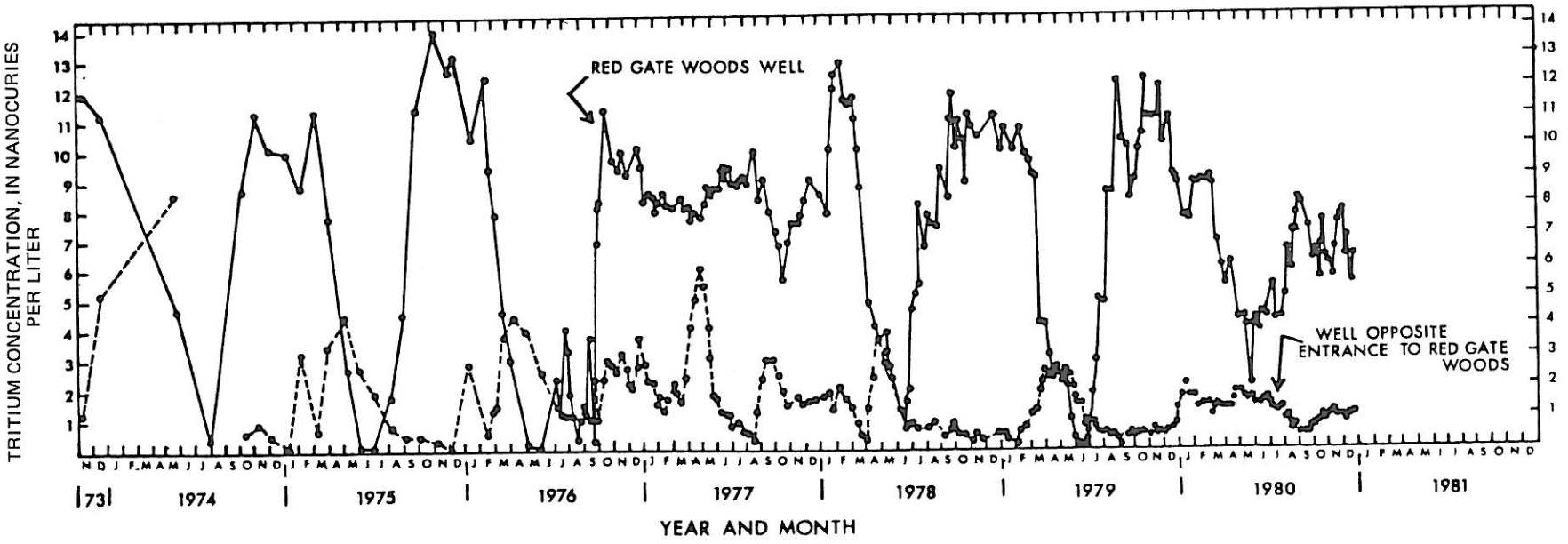

Figure 3. Tritium content of water from the Red Gate Woods well (forest preserve well 5167) and from the well (forest preserve well 5159) opposite the Red Gate Woods well next to the Illinois and Michigan Canal.

Table 1. Test-well construction data and lithologic description of cores of test well 26 at Plot M

COMPLETION DATE: October 9, 1979
LOCATION: 10 m northeast of the northeast corner of Plot M
SITE- AND WELL-CONSTRUCTION DATA (Values are in meters):

Altitude of land surface---------- 210.77
Altitude of measuring point (top of casing)--------- 210.99
Depth of bottom of piezometer from land surface----- 18.22

Type of piezometer: 1.22-m slotted PVC-pipe, 5.08-cm diameter

Unit No.	Sample No.	Depth interval (m)	Blow counts[1]	Recovery (cm)	Description
1	79S221	0- 0.46	8-12-15	15.2	Brown stony clay soil
1	79S222	0.46- .91	11-10-18	15.2	Brown clayey soil, root tubes, plant fragments
1	79S223	0.91- 1.37	20-20-24	25.4	Brown clayey soil with stones, plant fragments; 2.5-cm dry yellow sand layer at 1.16 m
1	79S224	1.37- 1.83	13-18-21	25.4	Yellow-brown silty clay with pebbles, mottled, hard, dry, flaky, brittle
1	79S225	1.83- 2.29	23-25-29	25.4	Yellow-brown silty clay with pebbles (large variety), flaky, brittle; plant fragments, Fe oxidation, pyrite; 45° fracture at 1.83 m
1	79S226	2.29- 2.74	14-20-25	61.0	Yellow-brown silty clay with pebbles (large variety); vertical fracture (25.4 cm) oxidized with plant debris
1	79S227	2.74- 3.20	14-20-26	45.7	Brown silty clay with pebbles, hard, dry
1	79S228	3.20- 3.66	20-21-25	40.6	Brown silty clay with pebbles, hard, dry; wet spot at 2.35 m; moist vertical fracture at 3.51 m
1	79S229	3.66- 4.12	9-11-15	35.6	Brown silty clay with pebbles, soft, moist, mottled; Fe oxidation
1	79S230	4.12- 4.57	7- 7-10	35.6	Brown silty clay with pebbles, soft, moist, mottled; Fe oxidation
1	79S231	4.57- 5.03	11-13-13	30.5	Brown silty clay, soft, moist, mottled
1	79S232	5.03- 5.49	9-13-18	50.8	Brown silty clay, soft, moist
1	79S233	5.49- 5.94	24-27-27	50.8	Brown silty clay, soft, moist; 5.1 cm water-bearing sand layer at 5.94 m
1	79S234	5.94- 6.40	13-19-50	35.6	Brown silty clay; 30.5 cm water-bearing sand layer with stones at 6.10 m
1	79S235	6.40- 6.86	19-15-16	45.7	Watery sand to 6.55 m; contact with brown silty clay with pebbles and stones
1	79S236	6.86- 7.32	37-32-27	40.6	Brown clayey silt with pebbles and stones
1	79S237	7.32- 7.77	9-12-17	45.7	Brown clayey silt grading to brown-gray clayey silt with pebbles, mottled
2	79S238	7.77- 8.23	18-20-18	35.6	Brown-gray clayey silt with numerous pebbles and stones, moist; Fe oxidation
2	79S239	8.23- 8.69	11-13-18	30.5	Brown-gray clayey silt with pebbles, gritty
2	79S240	8.69- 9.14	35-40-18	--	---
2	79S241	9.14- 9.60	25-18-18	30.5	Brown-gray clayey silt with pebbles, gritty
2	79S242	9.60-10.06	12-13-16	40.6	Brown-gray clayey silt to 9.75 m; contact with dark gray clayey silt with pebbles, dry, hard, dense
2	79S243	10.06-10.52	10-15-19	30.5	Dark gray silt to 10.21 m; contact with brown silt with pebbles
2	79S244	10.52-10.97	12-15-17	40.6	Brown silt with few pebbles, gritty, clean
2	79S245	10.97-11.43	39-25-23	30.5	Brown silt with few pebbles, gritty, moist, dense
2	79S246	11.43-11.89	9-12-16	40.6	Brown clayey silt with pebbles, gritty; 5.1 cm oxidized zone at 11.43 m
2	79S247	11.89-12.34	12-11-13	25.4	Gray-brown clayey silt with pebbles, gritty, moist, soft
2	79S248	12.34-12.80	18-48-12	15.2	Gray-brown clayey silt
2	79S249	12.80-13.26	10-12-45	20.3	Wet, gravelly, clayey silt with pebbles
2	79S250	13.26-13.72	7- 8-11	40.6	Wet, gravelly, clayey silt grading to brown-gray clayey silt

Table 1. Test-well construction data and lithologic description of cores of test well 26 at Plot M—*Continued*

Unit No.	Sample No.	Depth interval (m)	Blow counts[1]	Recovery (cm)	Description
2	79S251	13.72-14.17	6-11-13	30.5	Brown-gray clay grading to pink-brown silt, moist, clean
2	79S252	14.17-14.63	5- 7-24	35.6	Pink-brown silt with stones, pebbles, clean
2	79S253	14.63-15.09	18-11-23	20.3	Pink-brown silt to 14.69 m; contact with brown silt; graded layers of silt and sand
2	79S254	15.09-15.55	10-14-26	40.6	Brown clayey silt with pebbles, gritty, moist, soft
3	79S255	15.55-16.00	26-22-22	40.6	Brown clayey silt grading to brown-gray clayey silt
3	79S256	16.00-16.46	10-20-21	35.6	Brown-gray clayey silt grading to gray-brown clayey silt with pebbles
3	79S257	16.46-16.92	15-24-50/4	35.6	Gray-brown clayey silt grading to silt with pebbles, rocks, soft, moist
3	79S258	16.92-17.37	26-20-20	--	Rocks
3	79S259	17.37-17.83	12-16-17	15.2	Gray-brown clayey silt with pebbles, mottled
3	79S260	17.83-18.29	19-15-16	30.5	Brown-gray clayey silt grading to gray clayey silt with pebbles, gritty, moist, soft
		EOB 19.81 m			

[1]The 18-in. metal sample tube is driven into the ground to collect a sample. The number of hits or blows it takes to drive the sampler each 6 in. into the ground is always recorded as a measure of the hardness of the material.

DRILLING AND SUBSURFACE EXPLORATION PROGRAM

Under Survey supervision, the ANL began construction of a network of monitoring piezometers in the drift in 1976. Ten piezometers were installed in test wells that were constructed to a maximum depth of 12 m (test wells 1–10, fig. 2). Core samples were collected from two test wells (wells 22, 23, fig. 2) drilled through the concrete cap of the burial site in 1977. In late 1977 and early 1978, nested piezometers were installed at wells 11 and 24. Well-completion data, length of core recovered, and the geologic log of each test well are given by Olimpio (1982). As an example, the log of test well 26 is given in table 1. Table 2 gives the well-completion information for four bedrock test wells (DH1–DH4, fig. 1) drilled near Plot M in 1976. A complete description of the techniques used to drill the pre-1979 wells, together with the results of the radionuclide analyses of all the core samples collected, is given by Golchert and Sedlet (1978).

All the test wells drilled before 1979 were either next to or downgradient from Plot M between the two intermittent streams that drain the site. Furthermore, all but a few of the piezometers were located in the upper 10–15 m of the drift. In September 1979 and June 1980, the Survey drilled 15 additional wells in an effort to expand and deepen the downgradient ground-water-monitoring network. A piezometer was installed in each test well (locations 25–30, 33–37, fig. 2, table 1). The 15 new piezometers, together with the pre-1979 piezometers, provide a monitoring grid delineated by two east-west lines (*A–A′*, *B–B′*, fig. 2) and three north-south lines (*C–C′*, *D–D′*, *E–E′*, fig. 2).

The geologic and hydrologic data obtained from the 15 new test wells were used to define the lithologic and stratigraphic characteristics of the drift, to locate the approximate position of the water table, and to determine the hydraulic head distribution of the saturated zone in the drift.

Three types of borehole geophysical logs were run on each test well: natural-gamma, gamma-gamma, and neutron-epithermal neutron (fig. 4). The logs, which qualitatively identify lithology, indicate borehole and casing conditions, and aid stratigraphic correlation, were used as follows:

1. The natural-gamma logs were used to aid identification of less-radioactive sand layers in the clay- and silt-rich drift. Log identification of sand layers made it possible to correlate sandy strata (and also silty or gravelly strata) from well to well and thus played an important role in determining drift stratigraphy at the site.
2. The gamma-gamma logs measured the drift's capacity to reduce and attenuate induced radiation. Bulk density decreases to the right on the logs shown in figure 4; therefore, the response to a layer of sand is opposite to that of the natural-gamma log. Although the gamma-gamma logs did not accurately measure

Table 2. Site and well-construction data of bedrock wells in the forest preserve near Plot M

WELL DH1

COMPLETION DATE: September 17, 1976

LOCATION: Site A, at the top of the ridge in the Palos Forest Preserve

SITE AND WELL-CONSTRUCTION DATA (Values are in meters):

Altitude of land surface	226.46
Altitude of measuring point (top of casing)	227.06
Depth to bedrock from land surface	51.81
Depth to bottom of casing from land surface	53.34
Depth to bottom of borehole from land surface	65.53

Type of casing: black steel, 12.7-cm diameter

WELL DH2

COMPLETION DATE: September 20, 1976

LOCATION: 160 m south of Plot M on the north side of the forest preserve road; near well 21

SITE AND WELL-CONSTRUCTION DATA (Values are in meters):

Altitude of land surface	219.79
Altitude of measuring point (top of casing)	220.39
Depth to bedrock from land surface	46.93
Depth to bottom of casing from land surface	48.77
Depth to bottom of borehole from land surface	61.26

Type of casing: black steel, 12.7-cm diameter

WELL DH3

COMPLETION DATE: September 23, 1976

LOCATION: 30 m north-northwest of the northeast corner of Plot M; near well 4

SITE AND WELL-CONSTRUCTION DATA (Values are in meters):

Altitude of land surface	207.08
Altitude of measuring point (top of casing)	207.68
Depth to bedrock from land surface	37.18
Depth to bottom of casing from land surface	39.01
Depth to bottom of borehole from land surface	52.73

Type of casing: black steel, 12.7-cm diameter

WELL DH4

COMPLETION DATE: September 28, 1976

LOCATION: Approximately 200 m north of Plot M next to forest preserve road

SITE AND WELL-CONSTRUCTION DATA (Values are in meters):

Altitude of land surface	205.64
Altitude of measuring point (top of casing)	206.24
Depth to bedrock from land surface	33.22
Depth to bottom of casing from land surface	35.35
Depth to bottom of borehole from land surface	85.34

Type of casing: black steel, 12.7-cm diameter

the thickness of the sand layers, because the radius of detection of the nuclear probe was greater than all but the thickest sand layers, they were useful in identifying the location of sand layers and determining the thickness of clay-silt units.

3. The neutron and gamma logs were used together to distinguish between free water occupying pore spaces in the drift and chemically bound water.

REGIONAL GEOLOGY

The preglacial bedrock surface in northern Illinois ranges in age from Ordovician to Silurian. The study area (fig. 1) is underlain by Silurian dolomite that crops out along the Des Plaines River valley and the Calumet Sag Channel.

The Plot M site is located in the rough, irregular terrain of the Wheaton Morainal Country; the site is underlain by two till sheets of Wisconsinan age, the Wadsworth Till and the Malden Till (Lineback, 1979).

In this paper the term "drift" refers to the ice-laid mixture of clay, silt, sand, and coarse debris constituting the till sheets beneath the site.

DRIFT AT PLOT M

Geology

The Plot M site is situated on an end moraine and is directly underlain by 25–30 m of clayey silt. This deposit, the Wadsworth Till Member of the Wedron Formation, contains thin lenses and layers of sand and gravel and overlies sandy silt and gravel of the Malden Till Member of the Wedron Formation (Willman and Frye, 1970). The total thickness of the glacial drift beneath the site varies from 25 to 45 m.

The core samples indicate that the physical properties of the drift are uniform horizontally over the site. However, vertical variations of properties, in particular, variations in lithology, grain-size distribution, and color, were observed within both the Wadsworth and Malden Tills. Moreover, these small-scale vertical changes in the character of the drift were observed consistently at all test wells.

Therefore, for convenience in describing the small-scale characteristics of the drift, the vertical variations in lithology, grain-size distribution, and color within each till sheet were used to subdivide the drift into seven lithostratigraphic units. The units are referred to, from the surface downward, as Units 1 through 7 (table 3). Units 1–5 represent the Wadsworth Till Member, and Units 6 and 7, the Malden Till Member.

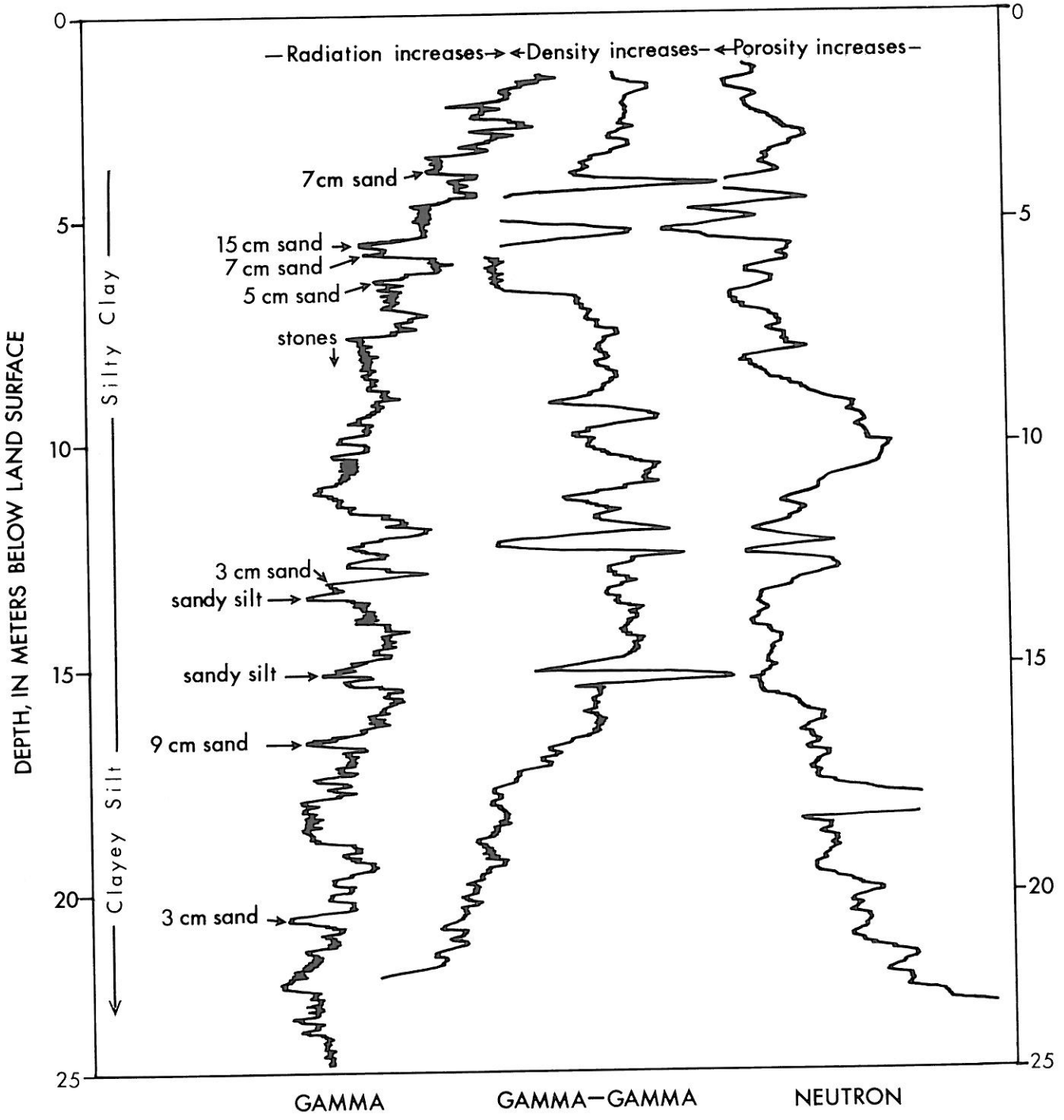

Figure 4. Comparison of three different geophysical logs to lithology in test well 28.

Lithology and Mineralogy

In general, the drift beneath the site is composed primarily of clay and silt, with smaller amounts of sand and gravel. The drift is an unsorted, mixed sediment in Unit 1; it becomes progressively better sorted, or layered, with increasing depth, particularly in Units 5–7. The color of the drift ranges from yellow-brown to light gray. Grain size ranges from clay-size to rocks as large as 8 cm in diameter.

Grain-size distribution of samples of the drift, as determined by hydrometer and sieve analyses, is shown in

Table 3. Geologic time-stratigraphic classification, rock stratigraphic classification, and general description of the drift at the Plot M site

System	Series	Stage	Substage	Formation	Member	Unit (this report)	Depth (m)	Thickness (m)	Description
						1	5	5	Yellow-brown silty clay containing pebbles; wide variety of mineral and rock fragments, oxidized fractures, discontinuous sand layers
						2	10	5	Alternating sequence of brown and gray-brown clayey silts containing pebbles and rocks; mostly dolomite and black shale grains, discontinuous sand and gravel layers
					Wadsworth Till[1]	3	15	5	Alternating sequence of brown and gray-brown clayey silts containing pebbles; mostly dolomite and black shale grains, relatively low density, easy to drill and sample
Quaternary	Pleistocene	Wisconsonian	Woodfordian	Wedron		4	20	5	Alternating sequence of gray and gray-brown silts, few or no pebbles; very dry and hard, relatively high density, difficult to drill and sample
						5	25	5	Gray and light gray silt and sand, no pebbles, dry, stiff, brittle, extremely hard, difficult to drill and sample
						6	30	5	Gray-brown gravelly sandy silt, moist, all grains are dolomite
					Malden Till[1]	7	35	5-7	Dark brown gravelly, clayey silt containing pebbles, moist; encountered only in test well 36
Silurian	Niagaran						40	50	

[1]Willman and Frye, 1970.

table 4. The samples were collected in the upper 35 m of the drift, corresponding with Units 1–6. The data in table 4 are arranged in order of descending altitude, or increasing depth. The average grain-size distribution for glacial moraines (undifferentiated) in the Wadsworth Till Member is shown for comparison.

The data show that each unit contains a distinct distribution of clay, silt, and sand. Unit 1 is relatively fine grained and is composed of more than 75 percent clay and silt. Units 2 and 3 are also composed chiefly of clay and silt; however, the proportion of silt increases with respect to clay, and the sand content is lower than that in Unit 1.

Table 4. Grain-size and composition data from samples of glacial drift at Plot M

Unit No.	Well No.	Sample No.	Altitude interval (m) Top	Bottom	Particle-size distribution (percentage of total amount) Sand[2]	Silt	Clay	Gravel	Clay minerals[1] (<0.004 mm fraction) Expandable clays	Illite	Chlorite/ Kaolinite
1	27	79S111	210.92	210.46	18	52	30	0	--	--	--
1	25	79S212	210.16	209.70	--	--	--	--	7	69	24
1	27	79S113	210.01	209.55	65	25	10	10	--	--	--
1	26	[3]79S227	208.03	207.57	11	48	45	0	18	62	20
1	26	79S227	208.03	207.57	10	58	32	0	18	62	20
1	28	79S2	207.78	207.32	--	--	--	--	17	59	23
1	28	79S3	207.32	206.88	--	--	--	--	13	58	29
1	27	79S110	206.81	206.35	25	40	35	0	--	--	--
1	29	79S5	206.41	205.95	--	--	--	--	14	72	14
1	26	79S233	205.28	204.82	17	53	30	--	4	74	22
1	27	79S125	204.52	204.06	15	62	23	0	--	--	--
1	29	79S59	203.60	203.15	25	50	25	14	--	--	--
1	28	79S12	203.21	202.75	--	--	--	--	5	75	20
1	25	79S217	202.38	201.93	9	72	19	4	--	--	--
2	27	79S132	201.32	200.86	16	34	50	0	--	--	--
2	27	[3]79S133	200.86	200.41	15	58	26	9	--	--	--
2	27	79S133	200.86	200.41	27	50	23	0	--	--	--
2	27	79S243	200.71	200.25	20	51	28	2	2	70	28
2	29	[3]79S66	200.40	199.95	13	46	41	3	--	--	--
2	29	79S66	200.40	199.95	26	47	27	0	--	--	--
2	28	79S19	199.64	199.18	13	45	42	0	--	--	--
2	29	79S69	199.03	198.57	28	49	23	0	--	--	--
2	27	79S138	198.58	198.12	--	--	--	--	7	65	28
2	27	79S141	197.21	196.75	3	70	27	0	42	32	26
2	26	79S251	197.05	196.60	--	--	--	--	7	66	27
2	28	79S25	196.90	196.44	23	39	38	0	--	--	--
2	30	[3]79S175	196.44	195.99	30	53	17	16	--	--	--
2	30	79S175	196.44	195.99	31	47	22	--	--	--	--
2	30	79S176	195.99	195.53	--	--	--	--	47	20	33
2	27	79S144	195.84	195.38	43	46	11	8	--	--	--
2	29	79S79	194.46	194.00	8	31	61	0	--	--	--
2	28	79S34	192.78	192.32	18	48	34	0	--	--	--
3	26	79S256	194.77	194.31	15	46	39	0	--	--	--
3	29	79S82	193.09	192.63	16	59	25	3	3	69	28
3	27	79S151	192.63	192.18	8	78	13	3	--	--	--

Table 4. Grain-size and composition data from samples of glacial drift at Plot M—*Continued*

Unit No.	Well No.	Sample No.	Altitude interval (m) Top	Bottom	Particle-size distribution (percentage of total amount) Sand[2]	Silt	Clay	Gravel	Clay minerals[1] (<0.004 mm fraction) Expandable clays	Illite	Chlorite/ Kaolinite
3	27	79S37	191.41	190.95	8	47	45	0	--	--	--
3	29	79S87	190.80	190.35	--	--	--	--	20	55	25
3	29	79S88	190.35	189.89	11	61	28	0	--	--	--
3	27	79S156	190.35	189.89	13	66	21	0	--	--	--
3	30	79S188	190.20	189.74	11	61	28	0	--	--	--
3	36	80S235	190.05	189.59	3	63	36	0	--	--	--
3	30	79S189	189.74	189.28	--	--	--	--	27	45	28
3	30	79S190	189.28	188.82	9	40	51	0	3	69	28
3	28	79S42	189.12	188.67	5	40	55	0	--	--	--
3	28	79S44	188.21	187.75	15	29	56	0	--	--	--
3	29	79S96[3]	186.69	186.23	20	62	18	0	--	--	--
3	29	79S96	186.69	186.23	11	71	16	11	--	--	--
4	36	80S239	188.21	187.76	11	33	56	0	--	--	--
4	30	79S195	187.00	186.54	--	--	--	--	6	67	27
4	29	79S103	183.49	183.03	12	70	18	0	6	67	27
4	30	79S203	183.34	182.88	2	81	17	0	--	--	--
4	30	79S205	182.43	181.97	4	76	20	0	--	--	--
4	30	79S207	181.24	181.05	1	83	16	0	10	61	29
4	30	79S209	180.60	180.14	4	73	23	0	3	74	23
5	36	80S253	181.81	181.36	4	76	20	0	--	--	--
5	35	80S202	181.64	181.15	6	79	19	0	--	--	--
5	35	80S204	180.72	180.27	3	71	26	0	--	--	--
5	36	80S259	179.07	178.61	1	84	15	0	--	--	--
6	36	80S268	174.96	174.50	23	55	22	0	--	--	--
6	36	80S269	174.50	174.04	24	52	24	0	--	--	--
Wadsworth Till Member of the Wedron Fm.[4]					16	27	57	--	--	--	--

[1]Identified by qualitative X-ray analyses.

[2]Hydrometer and sieve analysis: silt-clay boundary 0.004 mm, sand-silt boundary 0.062 mm.

[3]Duplicate analyses by separate laboratories.

[4]From Willman and Frye (1970, p. 168); data are percentages of whole sample; gravel is included in the sand determination.

Units 4 and 5 are composed chiefly of silt; very low sand content is an important characteristic of both units. Unit 6 is identified by approximately equal amounts of sand and clay mixed with silt.

Although sand layers within each unit account for only a small portion of the total volume of the drift, they are distinctive lithologically. The sand and gravel content of sample 79S113 (table 4) from a sand layer in Unit 1 exceeds 65 percent. Similarly, the sand and gravel content of sample 79S144 in Unit 2 is greater than 50 percent.

The predominant clay mineral in the drift is illite; it is accompanied by minor amounts of chlorite and expandable clays, notably montmorillonite, which were not detected clearly by X-ray analysis. These data agree with the analyses of Willman, Glass, and Frye (1963), who have shown that the illite-bearing late-Wisconsinan-age glacial deposits contain less than 5 percent montmorillonite.

The composition of grains in the drift larger than sand size is highly variable. In Unit 1, for example, a wide variety of highly weathered clastic, carbonate, and crystalline pebbles occurs in a clay-rich matrix. Petrographic analyses of drift thin sections have identified many detrital minerals, including quartz, biotite, muscovite, chlorite, plagioclase feldspar, K-feldspar, calcite, dolomite, pyrite, and several opaque minerals. Rock fragments in Unit 1 include quartzite, dolomite, black and green shale, and weathered igneous and (or) metamorphic rock.

Below Unit 1, the composition of the pebbles and rocks in the drift is less variable. Dolomite, black and green shale, and quartzite grains are most common. Pyrite occurs in the drift in Units 1–4.

Lithostratigraphy

The lithostratigraphic sequence within the drift was determined chiefly from the geologic properties of the drift described above. Interstratified sand layers and lenses were used to identify individual units and, in places, to mark the contacts between units.

Natural-gamma logs distinguished sand layers within the clay- and silt-rich units and also indicated sandy and gravelly zones within the drift. The logs further aided lithologic correlation of units between test wells. A cross section through well sites 4, 5, and 11 (fig. 5) demonstrates the use of the logs for correlation purposes by showing the identification and correlation of sand layers in Units 1, 2, and 3. The logs support the geological data in several ways:

1. Correlation of low-intensity (sand) peaks, in the middle of Unit 2, for example, indicates that the units (and thus the till sheets) are not horizontal, but dip slightly to the north and west.
2. Highest radiation intensity (the highest clay content) is measured in Unit 1, and this agrees with the grain-size-distribution data. Clay content of the drift decreases with increasing depth in Unit 1 and seems to be relatively constant throughout Unit 2.
3. The natural-gamma logs show that the sand layers are variable in thickness and in some places are discontinuous from well to well. For example, in test well 5, the response of the log to a prominent sand layer in the middle of Unit 2 is much less, and of slightly lower intensity, than the response of the log of test well 4 to the same layer. The log of test well 11 indicates that the same sand layer extends at least as far south as well 11; however, the geologic log of the well is incomplete, and thus the presence of the sand layer cannot be confirmed. Several low-intensity peaks in Unit 2 indicate sandy zones in the clay-silt sediment.
4. The logs are an indication of the degree of sorting of the sediments making up the drift. In Unit 1, the small, uniform peaks on the log (test well 11) indicate the uniform distribution of natural-gamma emitters, as represented by the clay content in the drift. Conversely, the log of Unit 2 is less uniform and displays three prominent low-intensity peaks. The log reflects geologic data indicating that the sediments in Unit 2 are better sorted and contain less clay than the sediments in Unit 1.

The stratigraphy of the drift beneath Plot M is illustrated in five geologic sections shown in figures 6, 7, 8, 9, and 10. As indicated in figure 2, there are three north-south sections: (1) section *E–E′* (fig. 6) is east of the burial ground, (2) section *D–D′* (fig. 7) passes through the burial ground, and (3) section *C–C′* (fig. 8) is west of the burial ground. There are two east-west cross sections: (1) section *B–B′* (fig. 9) is several meters north of the burial ground, and (2) section *A–A′* (fig. 10) is approximately 50 m north of the burial ground.

In the following discussion the specific lithostratigraphical, sedimentological, and structural characteristics of the Wadsworth and Malden Till Members of the Wedron Formation are described in detail. The purposes of the detailed description are to summarize the geologic data given in table 1 and to emphasize those characteristics of the drift that were most useful in subdividing the till members into Units 1–7.

Unit 1 is a yellow-brown silty clay that contains pebbles. The unit is approximately 5 m thick and is covered by 10–30 cm of topsoil. Samples of the clay are relatively dry and hard and display color mottling owing to oxidation. A water-bearing sand layer, ranging in thickness from 6 to 30 cm, is located in the middle of the unit in the area containing test wells 4, 26, 28, 29, 34, 35, 36, and 37. Thin, less continuous sand layers are present both above and below the large sand layer in the middle of Unit 1. Vertical and inclined fractures occur in the drift; however, only a small number of fractures were encountered. Sand and plant debris commonly fill the fractures,

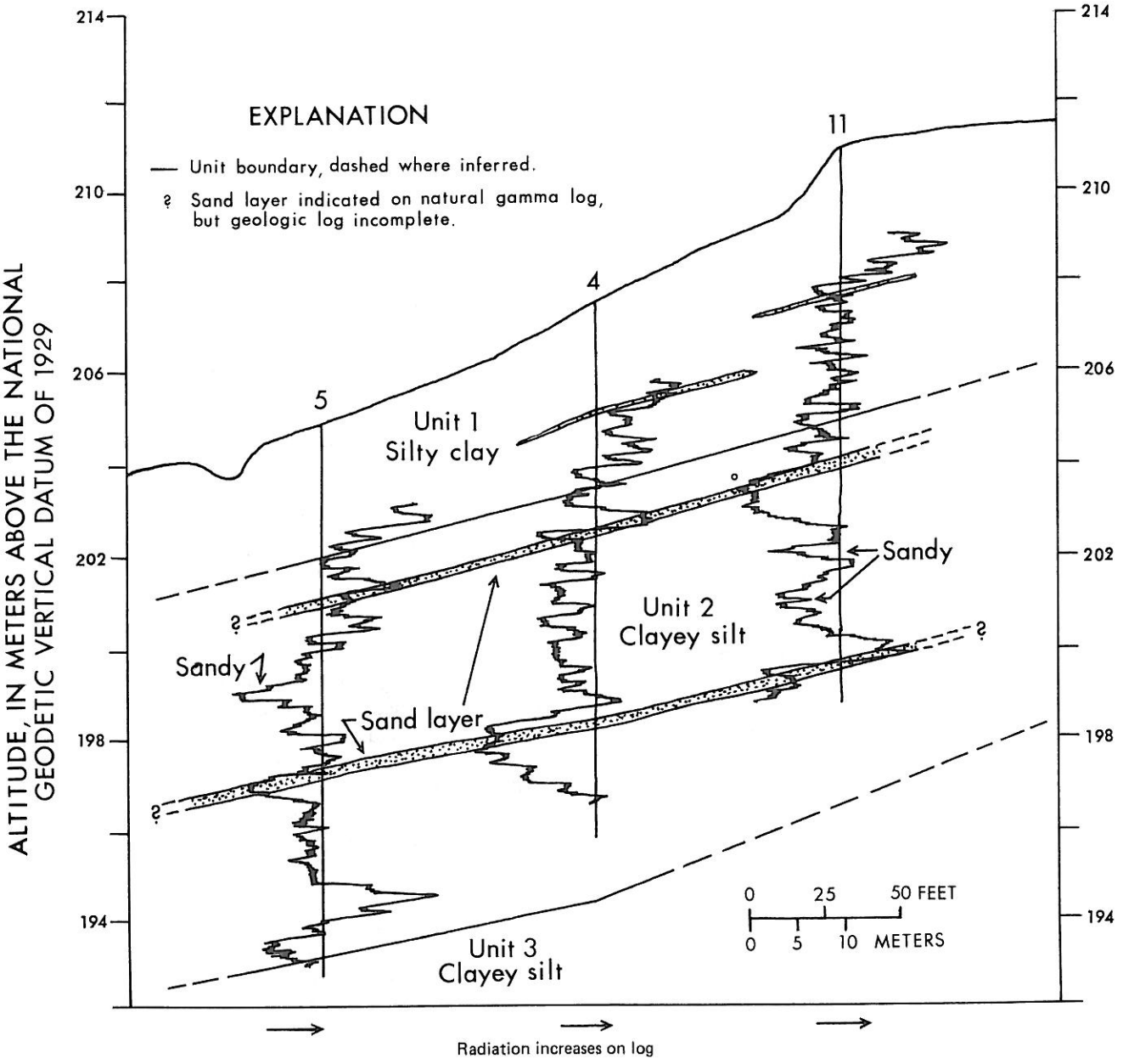

Figure 5. Correlation of natural-gamma logs from test wells 4, 5, and 11.

and oxidation of the adjacent drift is typical. Single fractures predominate in most 100-cm samples; frequency and spacing of fractures could not be determined by the vertical drilling method. The Unit 1/Unit 2 boundary is marked by a change from brown, sandy, silty clay to gray-brown clayey silt.

An alternating sequence of thin brown silts and gray-brown clayey silts 5 m thick constitutes Unit 2. The clayey silts contain numerous pebbles and rocks. Three lithologic layers within the unit are distinctive: (1) a dark-gray silty clay layer ranging in thickness from 6 to 20 cm approximately 2–3 m below the Unit 1/Unit 2 contact; (2) a gravelly, sandy silt layer ranging in thickness from 2 to 30 cm near the middle of the unit; and (3) a unique pinkish-brown layer ranging in thickness from 10 to 25 cm located 1–2 m below the gravel layer. These three layers occur beneath most of the Plot M site. The Unit 2/Unit 3 boundary is gradational; however, it is most often marked by the contact between a soft, brown gravelly silt and a gray-brown clayey silt.

Unit 3 is an alternating sequence of brown and gray-brown clayey silts; it closely resembles Unit 2, but Unit 3 is more silty. Unit 3 is 4–5 m thick. It contains a few pebbles, and sand layers and thin sand partings are numerous. Gamma-gamma logs indicate that the sediments in Unit 3 are less dense than those in either the overlying or the underlying units. The Unit 3/Unit 4 boundary is marked by a transition from soft, brown silt to gray-brown silt containing a few pebbles.

Gamma-gamma logs of Unit 4 show an increase in density and a decrease in porosity relative to Unit 3. Unit 4 is dense, hard, brittle, gray and gray-brown silt that contains few dolomite and black shale pebbles and only a small number of thin sand partings. Gamma-gamma logs

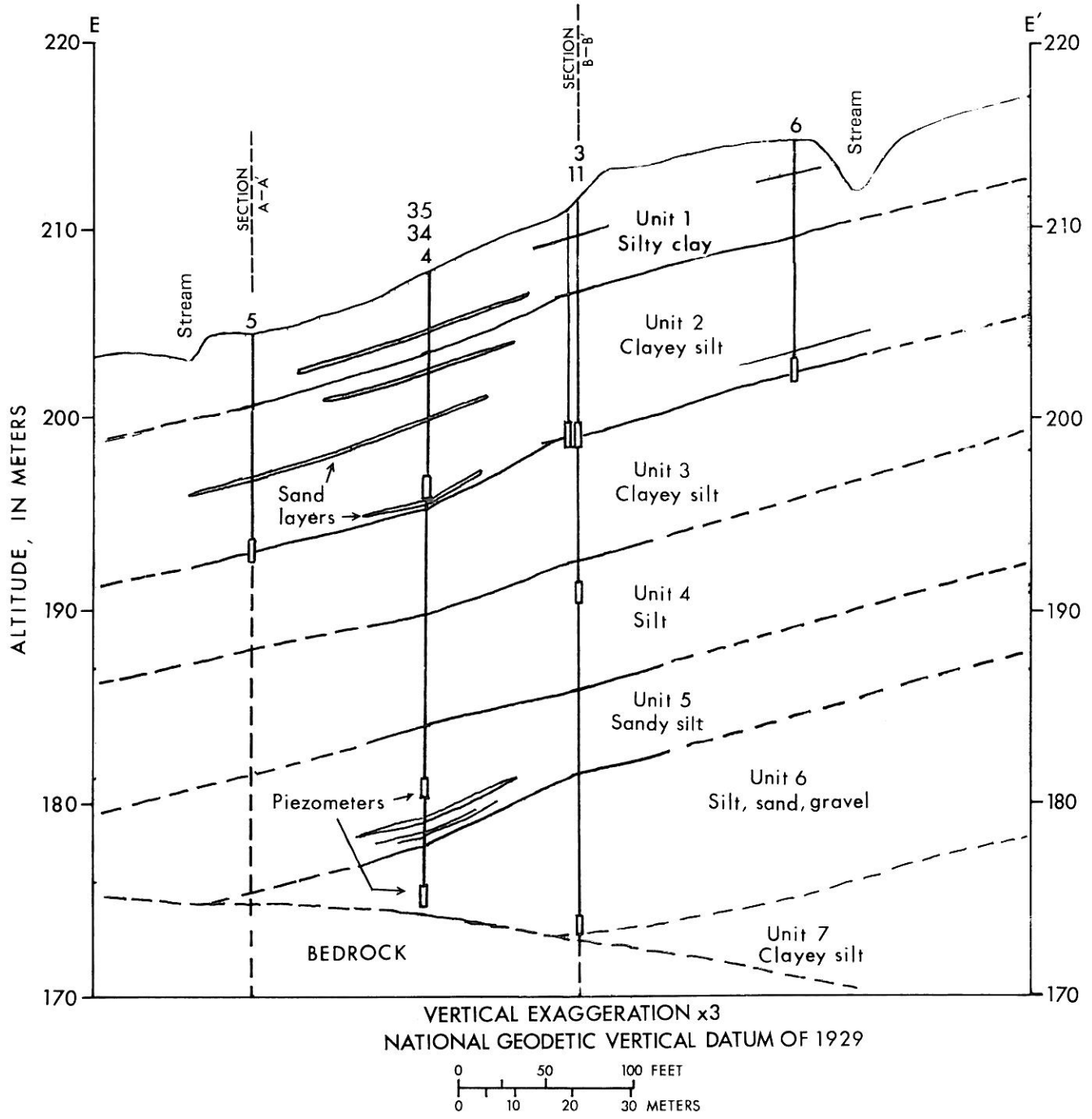

Figure 6. Geologic section *E–E'* of the Plot M site. Dashed lines represent approximate lithostratigraphic contacts in the drift.

show that the lower part of Unit 4 is the densest section of drift beneath the Plot M site. This 5-m-thick section of drift is a hard, dry silt that was very difficult to drill and sample.

Unit 5 is 4–5 m of gray and light-gray silt and does not contain pebbles. Core samples are hard, dry, and brittle. The Unit 5/Unit 6 boundary (the Wadsworth Till Member/Malden Till Member boundary) is marked by a distinctive black clayey silt (soil?) layer found in test wells 34 (by drilling only) and 36 and by a sharp change from light-gray silt to gray-brown gravelly silt.

Unit 6 bears little resemblance to the silt-rich sediments immediately overlying it. It is a gray-brown gravelly silt that ranges from 3 to 5 m in thickness and contains only dolomite pebbles. Samples are relatively soft, moist, and unconsolidated. Unit 7, encountered only as a thin zone in test well 36, is a dark-brown clayey silt also containing dolomite pebbles plus fragments of fresh

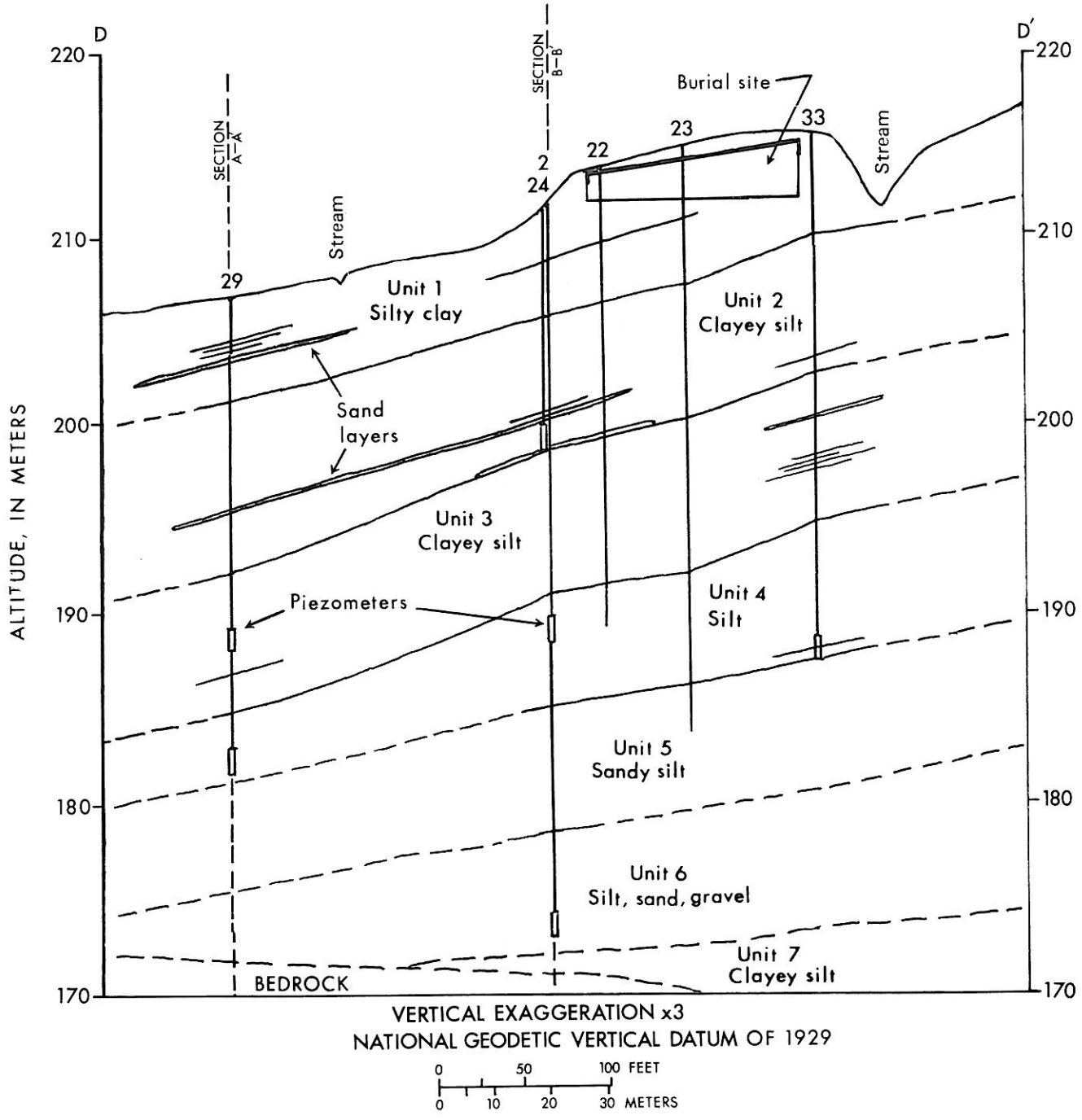

Figure 7. Geologic section *D–D'* of the Plot M site.

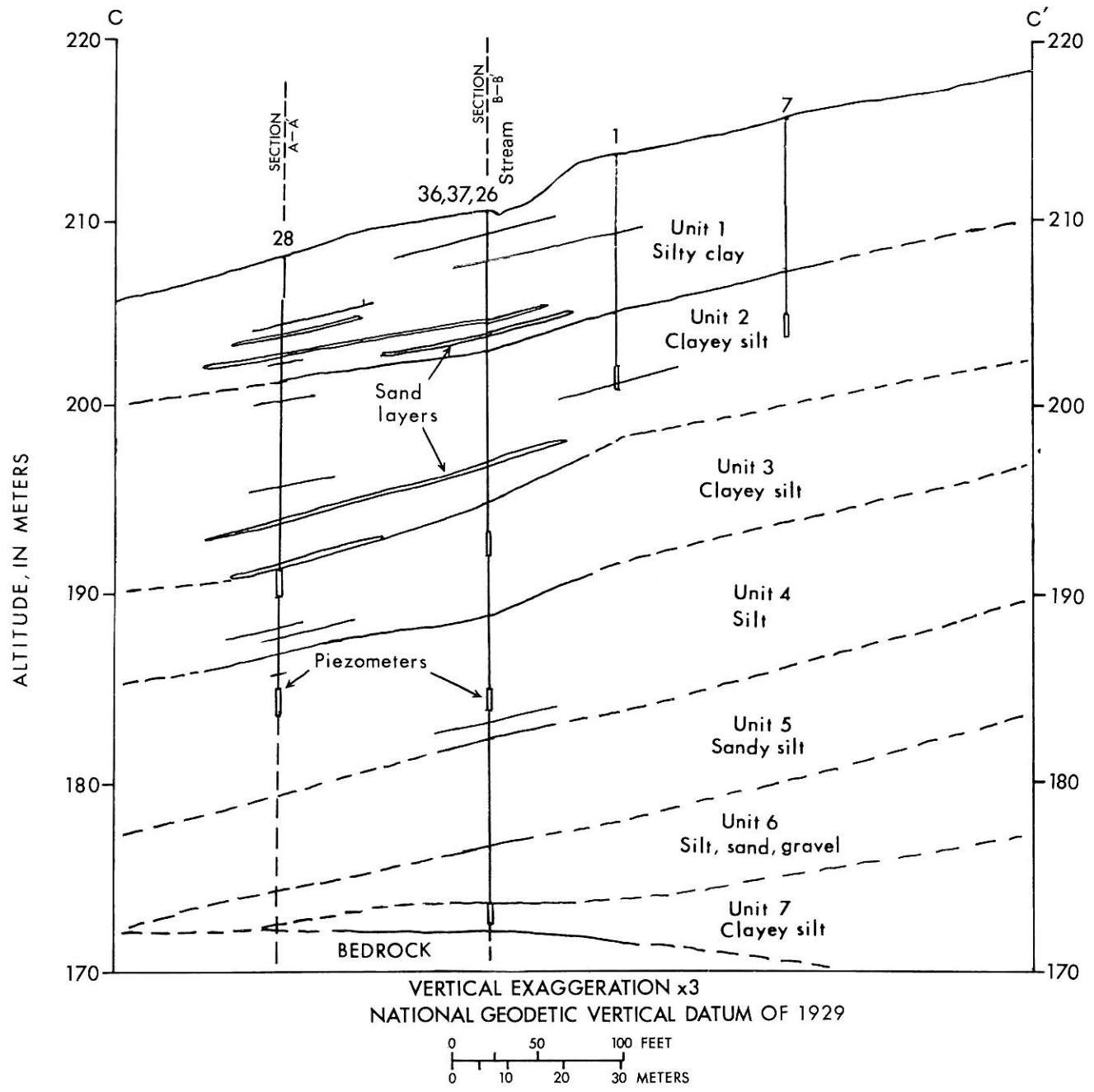

Figure 8. Geologic section *C–C′* of the Plot M site.

dolomite bedrock and layers of fine-grained dolomite sand.

Hydrogeology

Sources of Water

The amount and movement rate of water infiltrating the glacial drift depend largely on the number of water sources and their cumulative impact on the ground-water system. Water that comes in contact with the Plot M site derives from three main sources: (1) precipitation, (2) surface runoff from the surrounding hillsides, and (3) horizontal ground-water flow in the drift. The impact on the ground-water system from each of these sources is described below.

Precipitation

Precipitation data are available from the ANL, 6 km west of the forest preserve, and from Chicago's Midway Airport, 14 km northeast. The average annual precipita-

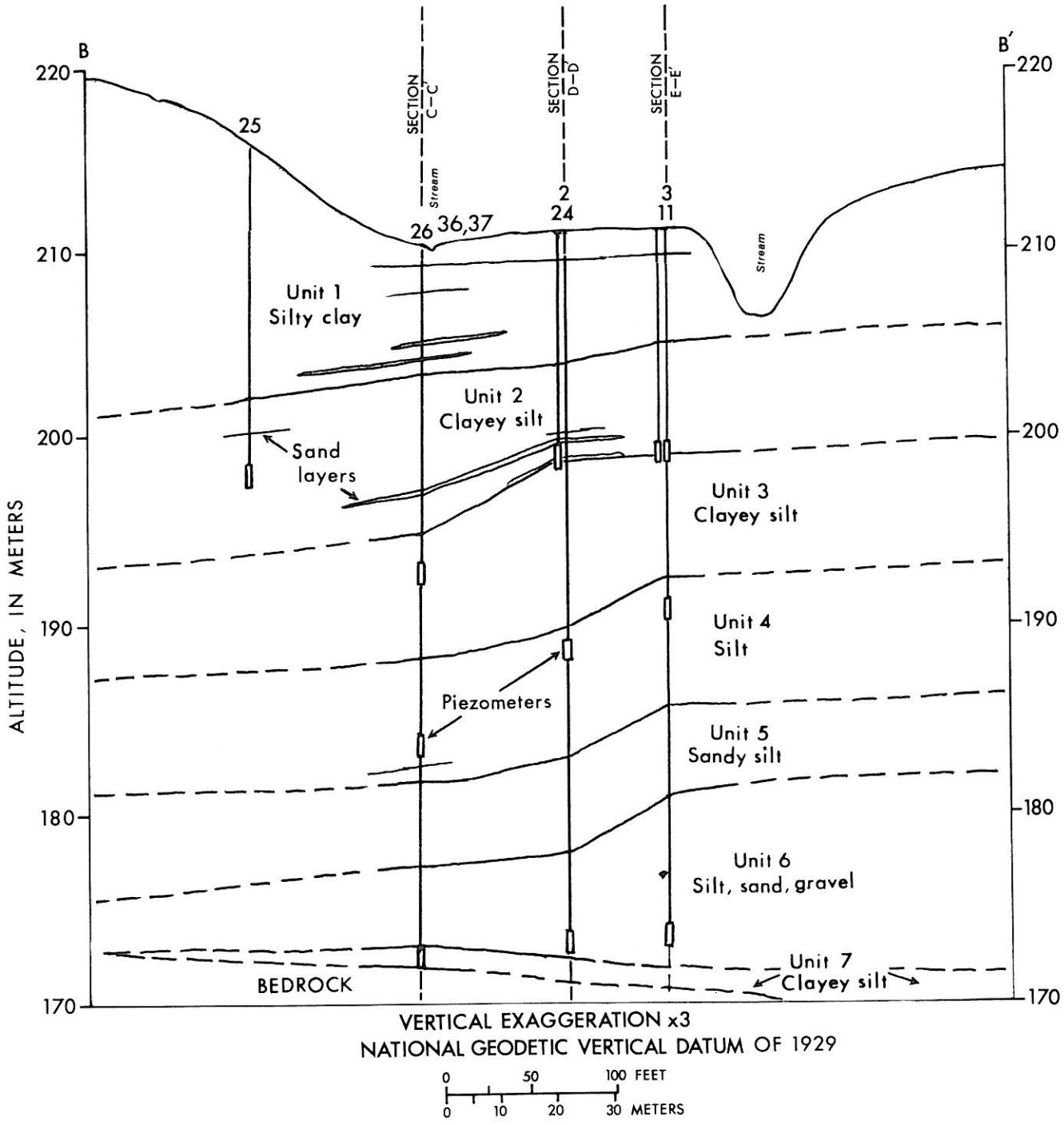

Figure 9. Geologic section *B–B'* of the Plot M site.

tion at Midway is approximately 85 cm. From 1950 to 1964, the average at the ANL was 80 cm; more recently (1970–80) this average increased to 93 cm. Precipitation at the ANL during the period 1976–80 is shown in figure 11.

Droughts are fairly common in the Upper Midwest. The 1976–77 drought was ranked in some midwestern States as one of the four worst since precipitation records were begun at the turn of the century (Matthai, 1979). In Illinois, the drought was somewhat less severe than in the

surrounding States. Precipitation at the ANL in 1976 totaled 77 cm, 83 percent of the annual average. Below-normal precipitation, streamflow, and ground-water levels persisted in Illinois from early 1976 to mid-1977 (Matthai, 1979).

Most of the precipitation at the forest preserve falls from April to September, during thunderstorms. Records show that 30–40 thunderstorm days occur annually and that on these days rainfall averages 3–5 cm. Snowfall averages 80 cm a year; however, accumulation of more than a few centimeters of snow at one time is rare. Nevertheless, the winters of 1977–78 and 1978–79 were the worst on record, bringing more than 200 cm of snowfall to the Chicago area each season.

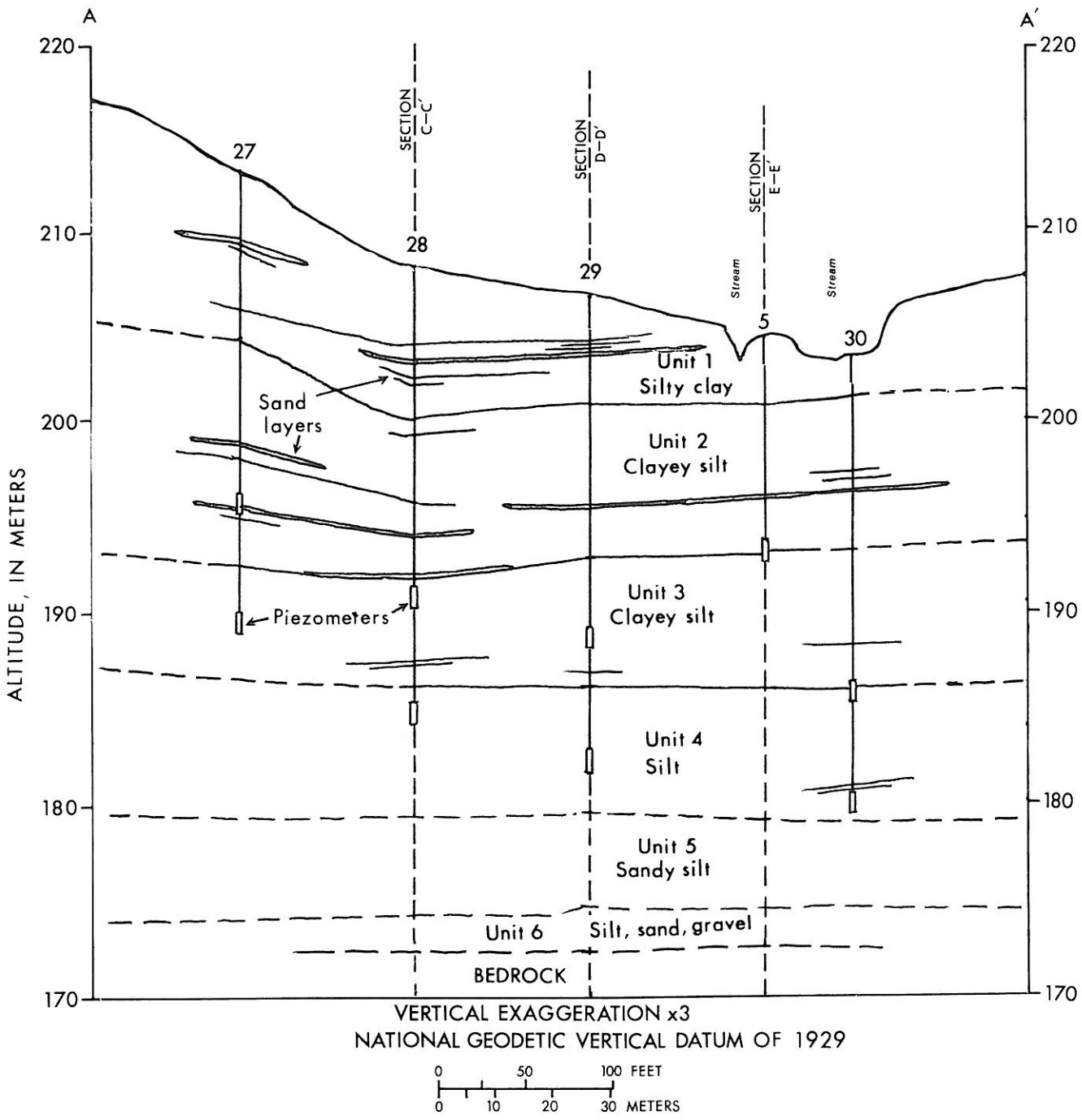

Figure 10. Geologic section *A–A'* of the Plot M site.

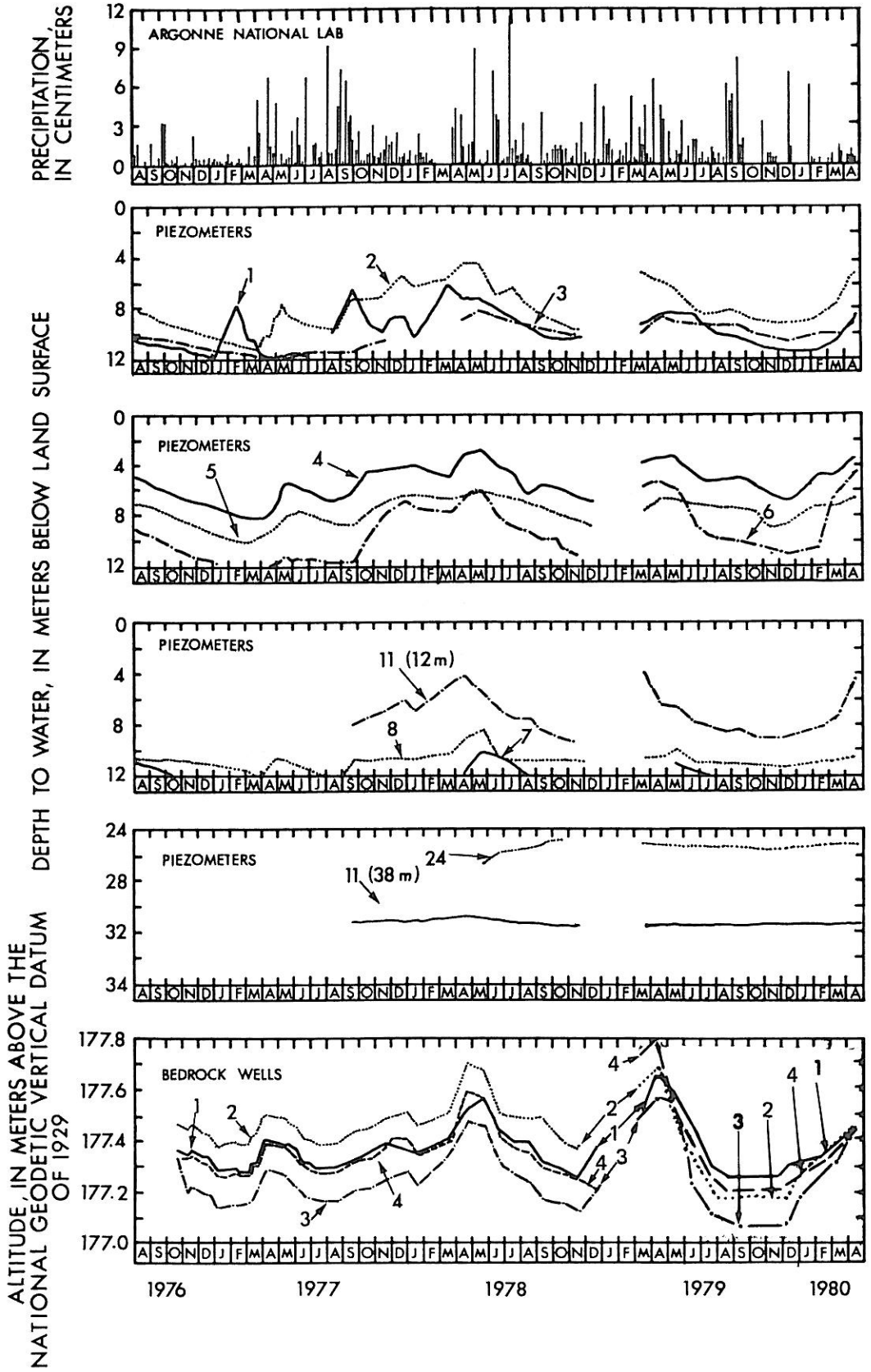

Figure 11. Monthly variation in precipitation and water levels in test wells at the Plot M site, August 1976 to April 1980.

The Plot M site is particularly vulnerable to water infiltration from precipitation in several ways:

1. It is an elevated open area resting against the side of a hill. Runoff from the higher hills to the west and south of the site is directed toward the open area. Severe storm runoff is directed to the site by a sloping access road.
2. Protective vegetation over the burial site consists of only a thin grass cover. Traffic over the site, particularly vehicular traffic, has periodically torn up the grass cover. Vandals have torn sod, made tire ruts, and burned the grass, all of which have contributed to accelerated erosion of the sod cover.
3. A deep ravine skirts the south and east sides of the site. The steep slopes are susceptible to channeling and erosion during heavy rainfall. Moreover, burrowing animals have taken advantage of the slopes to construct large open holes that slant toward the burial trenches.

Evapotranspiration

Evapotranspiration is the largest single component of water loss from the drift. It is the major factor that compensates for the effects of infiltration from precipitation and runoff directed toward the site. Evapotranspiration in the forest preserve is relatively high owing to the large area of dense vegetation, numerous swamps and wetlands, and the high average summer temperatures (20.0° to 22.8°C June to August, 1941–70, Midway Airport). In the forest preserve area, the average annual potential evapotranspiration is about 68 cm (Bloyd, 1975).

Local Runoff

Surface-water runoff from the burial site occurs only during periods of heavy rainfall. Erosion channels occasionally develop in the soil cover, especially where it has been rutted. The ravine on the east side and the ditch on the northwest side serve to drain storm runoff away from the Plot M site.

Ground-Water Flow

The abundance of water-bearing sand layers near the surface, the presence of inclined, stratified glacial deposits, and the occurrence of fractures may favor horizontal ground-water flow in the drift. At present, there is no direct evidence that lateral flow is transmitting water through the drift to the Plot M site; however, the hydraulic head data suggest that there is horizontal flow (see discussion below). Several sand layers and partings in Unit 1 underlie the burial trenches and appear to extend to the ravine east of the site and to the area north of the site, where the intermittent streams join. If the sand layers extend to the sides of the ravine upgradient from the site, surface water may infiltrate the soil cover and enter the layers.

Ground Water

The Unsaturated Zone

Neutron log data and moisture analyses of core samples show that the drift near the land surface is nearly, but not completely, saturated. Pore space in the clay-rich sediment is filled largely with water and to a smaller extent with air. This condition of the drift is termed either partially saturated or unsaturated.

In simple terms, the zone between the land surface and the water table is the unsaturated zone. The water table is the boundary between the unsaturated zone and the deeper saturated zone. Often, the ground-water system is more complex because of the occurrence of a capillary fringe above the water table. Thick capillary fringes are common in fine-grained sediments like those at Plot M.

At the midpoint of this study, few data have been compiled concerning the hydraulic properties of the unsaturated zone. The thickness and extent of the capillary fringe are unknown. Consequently, only a brief and general description of the characteristics of the unsaturated zone beneath Plot M is given here.

The unsaturated zone approximately corresponds to Unit 1. Laboratory analyses of the silty clay samples collected from Unit 1 show that moisture content ranges from 9 to 19 percent (cubic centimeter per cubic centimeter). The moisture content of fully saturated Unit 1 sediment samples is about 30 percent (tables 5, 6). Thus, the analyses show that Unit 1 is 30–60 percent saturated. These data clearly indicate the poor drainage characteristics of these tight clay-rich sediments. Moreover, these estimates are conservative because they do not take into account natural moisture loss during sample handling and laboratory testing.

Water table data were compiled primarily from drilling information gathered during construction of the well-monitoring network. The location of the water table was revealed by the level at which water was observed standing in the open borehole when first encountered during drilling. These data show that the Unit 1/Unit 2 boundary marks the average annual position of the water table. Furthermore, these data, together with information on annual variation of the drift, indicate that the average annual depth from the land surface to the water table ranges from 3 to 6 m.

The Saturated Zone

The saturated zone includes Units 2 through 7. In the upper part of the zone, all the piezometers in Units 2 and 3 (piezometers 1, 2, 3, 4, 5, 6, 7, 8, and 11; fig. 11) record seasonal water-level changes; the levels are highest

Table 5. Hydraulic conductivity of glacial drift at Plot M

A. PERMEAMETER DETERMINATIONS

Unit No.	Well No.	Sample No.	Altitude interval (m) Top	Bottom	Hydraulic conductivity (cm/s)	Direction	Average (cm/s)[1]	Total porosity
1	28	79S3	207.41	206.97	5.07×10^{-7}	Vertical		0.33
1	28	79S4	206.97	206.50	2.01×10^{-7}	Vertical	2.02×10^{-7}	.46
					1.83×10^{-7}	Vertical		.43
					2.23×10^{-7}	Vertical		.42
1	28	79S6	206.04	205.58	4.96×10^{-7}	Vertical		.41
1	28	79S7	205.58	205.12	2.01×10^{-6}	Vertical	1.61×10^{-6}	.36
					1.22×10^{-6}	Vertical		.32
1	27	79S122	205.89	205.43	1.12×10^{-6}	Vertical		.28
1	28	79S10	204.21	203.75	5.64×10^{-7}	Vertical		.33
1	28	79S11	203.75	203.30	6.39×10^{-7}	Vertical	8.84×10^{-6}	.34
					1.13×10^{-6}	Vertical		.32
1	26	79S237	203.45	203.00	7.37×10^{-6}	Vertical		.33
1	28	79S14	202.38	201.93	2.13×10^{-6}	Vertical	2.27×10^{-6}	.34
					2.40×10^{-6}	Vertical		.37
					1.44×10^{-6}	Horizontal		.37
1	30	79S163	201.93	201.47	2.38×10^{-6}	Vertical		.32
					1.12×10^{-6}	Horizontal		.31
1	29	79S63	201.78	201.32	8.72×10^{-7}	Vertical		.37
2	27	79S127	203.61	203.15	5.91×10^{-7}	Vertical	9.66×10^{-7}	.29
					1.34×10^{-6}	Vertical		.32
					5.36×10^{-6}	Horizontal		.34
2	36	80S223	201.93	201.48	1.34×10^{-6}	Vertical	1.23×10^{-6}	.29
					1.12×10^{-6}	Vertical		.29
2	26	79S242	201.17	200.71	1.26×10^{-6}	Vertical		.30
2	28	79S17	200.55	200.10	2.35×10^{-7}	Horizontal		.45
2	27	79S134	200.41	199.95	7.46×10^{-7}	Vertical		.32
2	27	79S138	198.58	198.12	3.33×10^{-6}	Vertical	4.41×10^{-6}	.34
					5.48×10^{-6}	Vertical		.34
2	27	79S139	198.12	197.66	3.20×10^{-6}	Vertical	2.92×10^{-6}	.30
					2.64×10^{-6}	Vertical		.31
2	26	79S250	197.51	197.05	7.99×10^{-7}	Vertical	9.10×10^{-7}	.32
					1.02×10^{-6}	Vertical		.31
2	29	79S73	197.20	196.75	6.13×10^{-7}	Vertical	7.50×10^{-7}	.34
					8.87×10^{-7}	Vertical		.32
2	30	79S30	195.99	195.53	2.74×10^{-6}	Horizontal		.33
2	30	79S176	195.99	195.53	2.74×10^{-6}	Horizontal		.33

Table 5. Hydraulic conductivity of glacial drift at Plot M—*Continued*

A. PERMEAMETER DETERMINATIONS--Continued

Unit No.	Well No.	Sample No.	Altitude interval (m) Top	Bottom	Hydraulic conductivity (cm/s)	Direction	Average (cm/s)[1]	Total porosity
2	30	79S177	195.53	195.07	1.95×10^{-6}	Vertical	1.89×10^{-6}	.29
					1.82×10^{-6}	Vertical		.30
2	28	79S27	195.98	195.53	1.53×10^{-6}	Vertical		.35
2	28	79S28	195.53	195.07	4.60×10^{-6}	Vertical		.36
2	28	79S29	195.07	194.61	4.79×10^{-6}	Vertical	5.89×10^{-6}	.30
					6.98×10^{-6}	Vertical		.37
2	36	80S227	195.84	195.38	7.36×10^{-6}	Horizontal		.33
2	28	79S30	194.61	194.15	1.78×10^{-6}	Vertical	1.99×10^{-6}	.32
					2.43×10^{-6}	Vertical		.27
					1.73×10^{-6}	Vertical		.36
					1.55×10^{-6}	Horizontal	1.67×10^{-6}	.32
					1.79×10^{-6}	Horizontal		.31
2	28	79S31	194.15	193.69	1.92×10^{-6}	Vertical	2.14×10^{-6}	.32
					2.35×10^{-6}	Vertical		.31
2	28	79S32	193.69	193.24	1.16×10^{-6}	Vertical	1.45×10^{-6}	--
					1.74×10^{-6}	Vertical		--
2	28	79S33	193.24	192.78	1.04×10^{-6}	Vertical		.32
3	35	80S181	191.24	190.78	1.02×10^{-6}	Vertical		.29
3	36	80S234	190.50	190.05	1.47×10^{-6}	Vertical	1.29×10^{-6}	.30
3	29	79S92	188.52	188.06	2.61×10^{-6}	Vertical	3.05×10^{-6}	.33
					3.49×10^{-6}	Vertical		.32
					2.74×10^{-6}	Horizontal	3.50×10^{-6}	.32
					4.26×10^{-6}	Horizontal		.31
3	29	79S93	188.06	187.60	2.19×10^{-6}	Vertical		.34
3	29	79S94	187.60	187.15	1.19×10^{-6}	Vertical		.33
					6.39×10^{-7}	Horizontal		.33
					1.11×10^{-6}	Vertical		.29
4	35	80S186	188.95	188.49	1.09×10^{-6}	Vertical		.30
					2.51×10^{-6}	Horizontal		.28
4	36	80S238	188.67	188.21	5.19×10^{-6}	Vertical	6.34×10^{-6}	.37
					7.49×10^{-6}	Vertical		--
4	36	80S254	185.47	185.01	2.07×10^{-6}	Vertical		.31
4	36	80S246	185.01	184.56	3.75×10^{-6}	Vertical	3.72×10^{-6}	.29
					3.69×10^{-6}	Vertical		.31
4	36	80S247	184.56	184.10	1.36×10^{-6}	Vertical		.31

Table 5. Hydraulic conductivity of glacial drift at Plot M—*Continued*

A. PERMEAMETER DETERMINATIONS--Continued

Unit No.	Well No.	Sample No.	Altitude interval (m) Top	Altitude interval (m) Bottom	Hydraulic conductivity (cm/s)	Direction	Average (cm/s)[1]	Total porosity
4	29	79S99	185.32	184.86	2.34×10^{-6}	Vertical	2.07×10^{-6}	.29
					1.79×10^{-6}	Vertical		.32
					8.78×10^{-7}	Vertical		.31
4	35	80S194	185.49	184.84	7.90×10^{-7}	Vertical		.26
4	36	80S294	183.64	183.19	3.03×10^{-6}	Vertical		.30
4	36	80S251	182.73	182.27	4.75×10^{-6}	Vertical		.33
					5.20×10^{-6}	Horizontal		.32
4	35	80S197	183.92	183.47	1.97×10^{-6}	Vertical	2.15×10^{-6}	.30
					2.32×10^{-6}	Vertical		.31
5	35	80S198	183.47	183.01	8.74×10^{-6}	Vertical		.32
5	35	80S205	180.27	179.81	1.10×10^{-6}	Horizontal		.31

B. PRESSURE PULSE DECAY DETERMINATION

Unit No.	Well No.	Sample No.	Altitude interval (m) Top	Altitude interval (m) Bottom	Hydraulic conductivity (cm/s)
1	25	79S212	210.16	209.7	2.20×10^{-8}
1	27	79S120	206.81	206.35	1.66×10^{-7}
1	29	79S59	203.60	203.15	1.38×10^{-8}
1	29	79S60	203.15	202.69	3.48×10^{-9}
3	27	79S156	190.35	189.88	1.05×10^{-7}
4	29	79S103	183.49	183.03	4.99×10^{-8}
4	30	79S204	182.88	182.43	2.88×10^{-7}

C. FIELD BAILER TESTS OF PIEZOMETERS

Unit No.	No. of tests	Hydraulic conductivity Mean (cm/s)	Hydraulic conductivity Median (cm/s)	Hydraulic conductivity Range (cm/s)
2	6	1.060×10^{-6}	2.050×10^{-7}	1.274×10^{-8} to 3.207×10^{-6}
3	2	1.040×10^{-7}	6.100×10^{-7}	1.933×10^{-8} to 1.887×10^{-7}

[1]Duplicate and triplicate analyses were performed on many (but not all) samples.

Table 6. Total porosity, bulk density, specific gravity, and surface-area data of samples of glacial drift at Plot M

Unit No.	Well No.	Sample No.	Altitude interval (m) Top	Bottom	Total porosity (percentage of volume)	Bulk density (gm/cm^3)	Specific gravity (gm/cm^3)	Surface area (m^2/gm)
1	27	79S111	210.92	210.45	26.9	2.20	2.72	40.6
1	25	79S212	210.16	209.70	31.9	2.17	2.76	--
1	26	[1]79S227	208.03	207.57	33.1	2.11	2.72	55.4
1	26	79S227	208.03	207.57	32.1	2.17	2.77	--
1	27	[1]79S120	206.81	206.35	29.9	2.22	2.77	30.0
1	27	79S120	206.81	206.35	30.9	2.23	2.83	--
1	29	79S59	203.60	203.15	27.9	2.26	2.73	--
1	29	79S60	203.15	202.69	25.8	2.28	2.73	--
2	29	[1]79S66	200.40	199.95	36.4	2.19	2.74	29.2
2	29	79S66	200.40	199.95	26.6	2.30	2.82	--
2	27	[1]79S133	200.86	200.41	26.7	2.22	2.70	26.3
2	27	79S133	200.86	200.41	27.8	2.27	2.80	--
2	29	79S69	199.03	198.57	25.5	2.28	2.75	14.5
2	27	79S142	197.21	196.75	27.3	2.24	2.71	--
2	30	[1]79S175	196.47	196.02	26.9	2.26	2.75	2.9
2	30	79S175	196.47	196.02	25.7	2.29	2.74	--
3	29	79S87	190.80	190.35	27.9	2.28	2.75	14.5
3	27	[1]79S156	190.35	189.88	27.2	2.46	2.72	18.8
3	27	79S156	190.35	189.58	27.0	2.24	2.69	--
3	29	79S96	186.69	186.23	22.2	2.40	2.75	14.4
4	29	[1]79S103	183.49	183.03	19.8	2.26	2.53	4.6
4	29	79S103	183.49	183.03	26.4	2.27	2.73	--
4	30	79S203	183.34	182.88	24.3	2.31	2.72	14.3
4	30	79S204	182.88	182.43	26.4	2.26	2.72	--
4	30	79S207	181.24	181.05	25.7	2.11	2.72	55.4

[1]Duplicate analysis of one sample performed in separate laboratories.

in April and lowest in November and December. Annual water-level changes in the piezometers range from 0.5 to 5 m. Piezometers 4, 5, and 6 contain the largest amounts of water and measure the greatest annual fluctuations. The responses of these piezometers are due chiefly to the variably saturated condition of the two sand layers nearby in Units 1 and 2.

Seasonal water-level changes, drainage and recharge of water during field tests, and annual fluctuations of tritium content in water in the near-surface piezometers indicate that the clay-rich sediments do indeed transmit water, but at a slow rate. A zone deeper down in the drift, approximately 10 m below the water table, seems to transmit water at extremely slow rates. This zone, ranging from 10 to 12 m thick and observed throughout the area of the Plot M site, extends from the top of Unit 4 to the bottom of Unit 5.

The most significant characteristic of Units 4 and 5 is that they do not yield water to wells. All the piezometers at the Plot M site positioned in the two units (at loca-

tions 11, 24, 27, 28, 29, 30, 33, 34, and 37) have remained dry since their installation. The absence of water may be due to the saturated condition of the predominantly silty sediments or to an effect related to the size of the piezometers. To better understand the hydraulic properties of this portion of the saturated zone in view of the present data, it is necessary to examine these alternative explanations in further detail.

The data show that the degree of saturation of Units 4 and 5 is not significantly less than that in the overlying and underlying water-yielding drift. Neutron moisture logs and core sample analyses show no difference in moisture content between Units 4 and 5 and Units 2, 3, 6, and 7. The hydraulic conductivity of all units, measured by field and laboratory techniques (described below; table 5), is relatively uniform. Furthermore, tritium has migrated into and through the zone to the underlying drift and bedrock. When summarized, the present data indicate that Units 4 and 5 are near saturation, transmit water, and have pressure heads that are close to zero, either positive or negative.

The absence of water in the piezometers may be attributed either to moisture evaporating as fast as it collects or to zero-to-slightly-negative pressure head. The large diameter of the piezometers, inaccurate for measurement of low pressure head, may compound the problem. The piezometers are carefully sealed from the land surface, and slug tests confirm that they are not plugged.

Hydraulic Conductivity

The hydraulic conductivity of the saturated drift was determined by application of two laboratory techniques (permeameter and pressure pulse decay) and by field tests. Data from bailer tests of piezometers in Units 2 and 3 were used to calculate horizontal hydraulic conductivity (table 5*C*). Six piezometers in Unit 2 yielded values ranging from 1.3×10^{-8} to 3.2×10^{-6} cm/s (centimeters per second) and two piezometers in Unit 3 yielded values of 1.9×10^{-8} and 1.9×10^{-7} cm/s. The average horizontal hydraulic conductivity in Units 2 and 3 is 6.1×10^{-7} cm/s; this composite value for the two units includes the effects of both sand layers and fractures near the piezometers.

A pressure pulse decay techique was used to determine the vertical hydraulic conductivity of seven core samples from Units 1, 3, and 4 (table 5*B*). This technique yielded very low values for these units, particularly for Unit 1. The permeameter data were obtained from samples of Units 1–5 (table 5*A*). The tests yielded hydraulic conductivity values that correspond more closely with the field-determined values. Moreover, the permeameter values are uniform. With only a few exceptions, the vertical and horizontal hydraulic conductivity values fall within the range 1×10^{-6} 9×10^{-6} cm/s.

Summarizing the hydraulic conductivity data, the pressure pulse method yields values 1 to 2 orders of magnitude lower than field test values. On the other hand, the permeameter values are slightly higher than the field values. The pressure pulse decay technique yields erroneously low values because the samples are squeezed by a small confining pressure during the lab test.

Total Head and Ground-Water Flow

The total hydraulic head field along cross-section *E–E′* is shown in figure 12. The section is parallel to the direction of primary ground-water flow (vertically downward) and to the direction of secondary flow (horizontally northward). The equipotential head lines are based on piezometer data gathered in May 1980, and the head gradients and flow directions illustrated in the section are representative of the hydraulic properties of the drift that have prevailed since the beginning of this study.

For the following discussion of flow in the drift, it is convenient to divide the total head field into two parts, an upper part characterized by a significant horizontal gradient and a lower part characterized by a vertical gradient.

In the upper part of the field, five piezometers (3, 4, 5, 6, and 11) record a 6-m decrease in total head from the south side of the site (piezometer 6) to the north side (piezometer 5). Although ground water moves primarily downward, a relatively large horizontal gradient occurs at the base of Unit 1 and throughout Unit 2. The horizontal gradient is caused by a combination of factors: (1) the gentle, northward dip of the strata, (2) numerous sand lenses in the two units, and (3) fracturing of the near-surface drift.

Units 4 and 5 strongly influence the head distribution in the lower part of the total head field. Equipotential head lines are alined parallel to the strata, and ground-water flow is vertically downward. The near-zero pressure head in Units 4 and 5 causes (1) low total head and a very small vertical gradient in both units, and (2) a sharp decrease in total head and a large gradient ("bundling") in overlying Unit 3. Equipotential lines at the base of the drift intersect the sloping-bedrock surface at a low angle.

→

Figure 12. Cross-section *E–E′* through the Plot M site showing the vertical hydraulic head distribution and principal ground-water flow direction—May 1980.

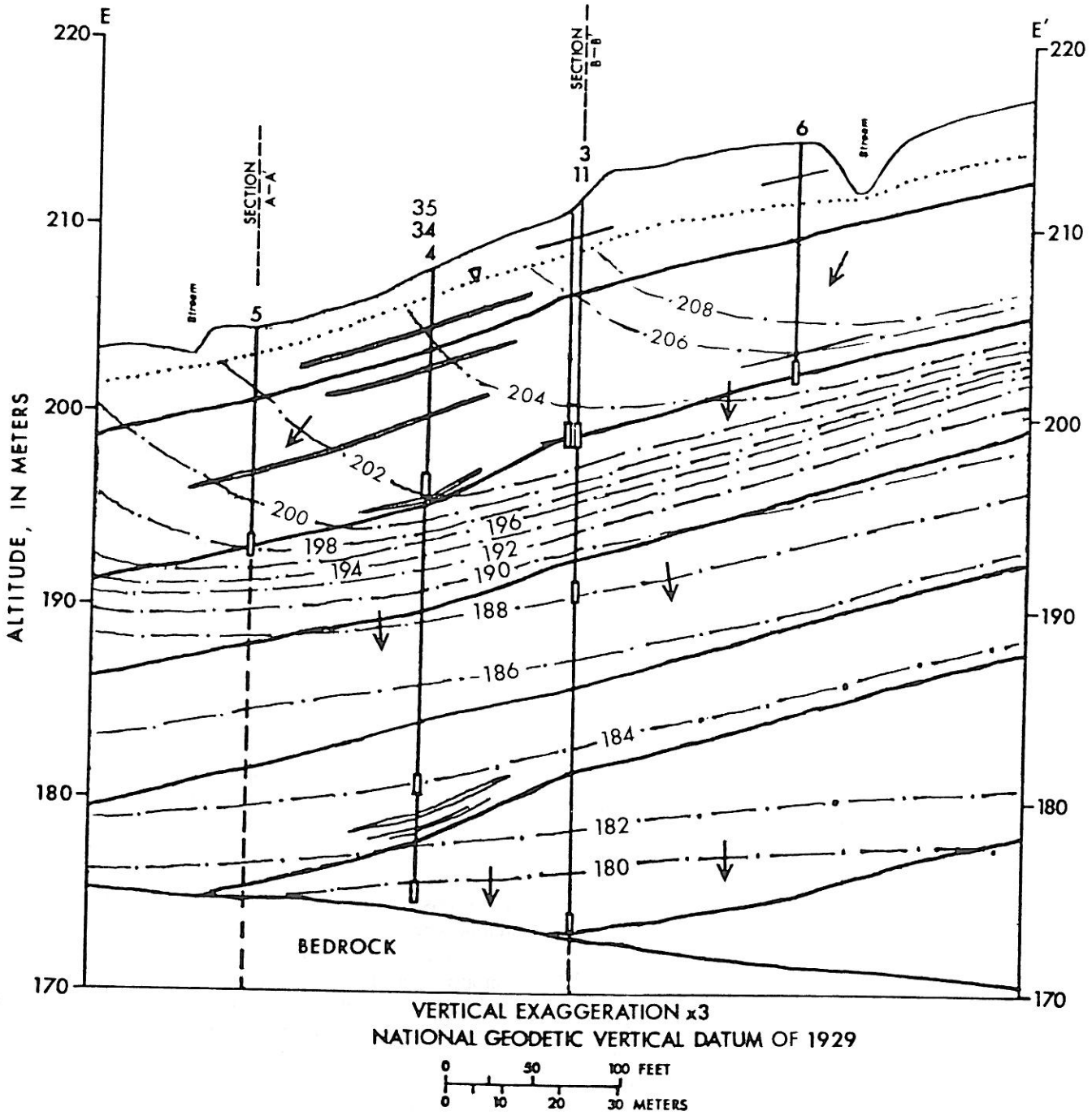
E
E'
220
210
200
190
180
170
ALTITUDE, IN METERS
SECTION A–A'
SECTION B–B'
Stream
Stream
5
35
34
4
3
11
6
208
206
204
202
200
198
196
194
192
190
188
186
184
182
180
BEDROCK
VERTICAL EXAGGERATION x3
NATIONAL GEODETIC VERTICAL DATUM OF 1929
0 50 100 FEET
0 10 20 30 METERS
EXPLANATION
6
Piezometer
Water table
Sand layer
180
Equipotential line, altitude in meters
Ground–water flow direction

GROUND WATER IN THE SILURIAN DOLOMITE

The hydrographs of water level for bedrock wells DH1–DH4 (fig. 11) show responses to spring recharge and summer recession as well as long-term trends associated with annual precipitation variations. Since 1976, water levels in these wells have generally risen as the ground water depleted by the drought of 1976 is replenished. The pattern of water-level fluctuations is similar in all wells, which indicates that the aquifer responds to stress in a uniform manner over the forest preserve area. No data on the hydraulic head distribution of the aquifer have been compiled.

TRITIUM MIGRATION

Studies at Plot M

Since 1976, the work effort to determine the extent of tritium migration at the Plot M site had been shared by the Survey and by the ANL. This study is primarily concerned with the aerial and vertical extent of subsurface migration in the glacial drift. The ANL performs radiometric analyses of both soil moisture extracted from core samples and water collected from wells. A discussion of the analytical techniques used, as well as a presentation of the results of the radiometric analyses of all soil and water samples collected during the period 1976–78, is given by Golchert and Sedlet (1978).

The Tritium Plume at Plot M

Tritium concentration levels measured in soil moisture from core samples collected up until June 1980 are illustrated on cross-sections *E–E′*, *B–B′*, and *A–A′* (figs. 13–15). Concentration levels are given in units of nanocuries per liter of water (nCi/L); lines of equal concentration indicate exponential changes in tritium concentration levels. For reference purposes, the lithostratigraphic unit boundaries and the positions of the piezometers are shown. In most areas, the lines of equal concentration are based on data derived from continuously collected core samples. In this paper, the contaminated volume, that is, the volume of the drift where tritium concentration levels exceed 10 nCi/L, is referred to as the tritium plume. For purposes of comparison, 3 nCi/L of tritium is the drinking water limit set by the U.S. Environmental Protection Agency (1973).

Section *E–E′*

North-south cross-section *E–E′* shows the maximum lateral and vertical extent of the tritium plume. The plume extends laterally from the ravine south of the site to the area north of test well 5 and vertically from the middle of Unit 1 to bedrock. Also, the plume narrows downward; in this section it decreases in width from more than 90 m in Unit 1 to less than 50 m at the bedrock surface.

At test well 11, highest concentration levels, exceeding 10,000 nCi/L, are measured in a zone extending from the Unit 1/Unit 2 boundary to the middle of Unit 5. Between test wells 11 and 35, tritium concentration levels higher than 1,000 nCi/L are measured in core samples collected from just above the bedrock surface.

The shape of the plume clearly indicates that the principal direction of tritium migration is vertically downward. Also, the lines of equal concentration bend laterally northward in several areas, forming several small, distinct "lobes." An upper lobe corresponds with the location of the water-bearing sand layers in the upper part of Unit 2. A middle lobe corresponds with the sand and gravel layers at the base of Unit 2, and a lower lobe extends northward in Unit 4. The upper and middle lobes are most distinctive and are associated with horizontal movement of tritiated water along the sand layers in Units 1 and 2.

Section *B–B′*

Cross-section *B–B′* shows the east-west extent of the tritium plume. As along section *E–E′*, tritium has migrated deeper into the drift than it has either to the east or to the west. Concentration levels are relatively low on the east side of the site beneath the ravine and on the west side beneath test well 25. The zone of highest concentration levels, exceeding 10,000 nCi/L, is confined to the area between the ravine and test well 26.

In a few zones in the drift, for example in this section at piezometer 2 located at the base of Unit 2, tritium concentration levels in soil moisture reach as high as 50,000 nCi/L. The geologic data show that the areas of very high tritium concentration are associated with sand layers. Conversely, low levels of tritium concentration in soil moisture east and west of the site are due in part to the small number of thin, dry sand layers in these areas.

Section *A–A′*

Cross-section *A–A′* is near the leading, north edge of the tritium plume. The cross-sectional area of the plume is small compared with the area of the plume directly below Plot M. Also, tritium concentration levels are significantly lower. The east-west width of the plume in

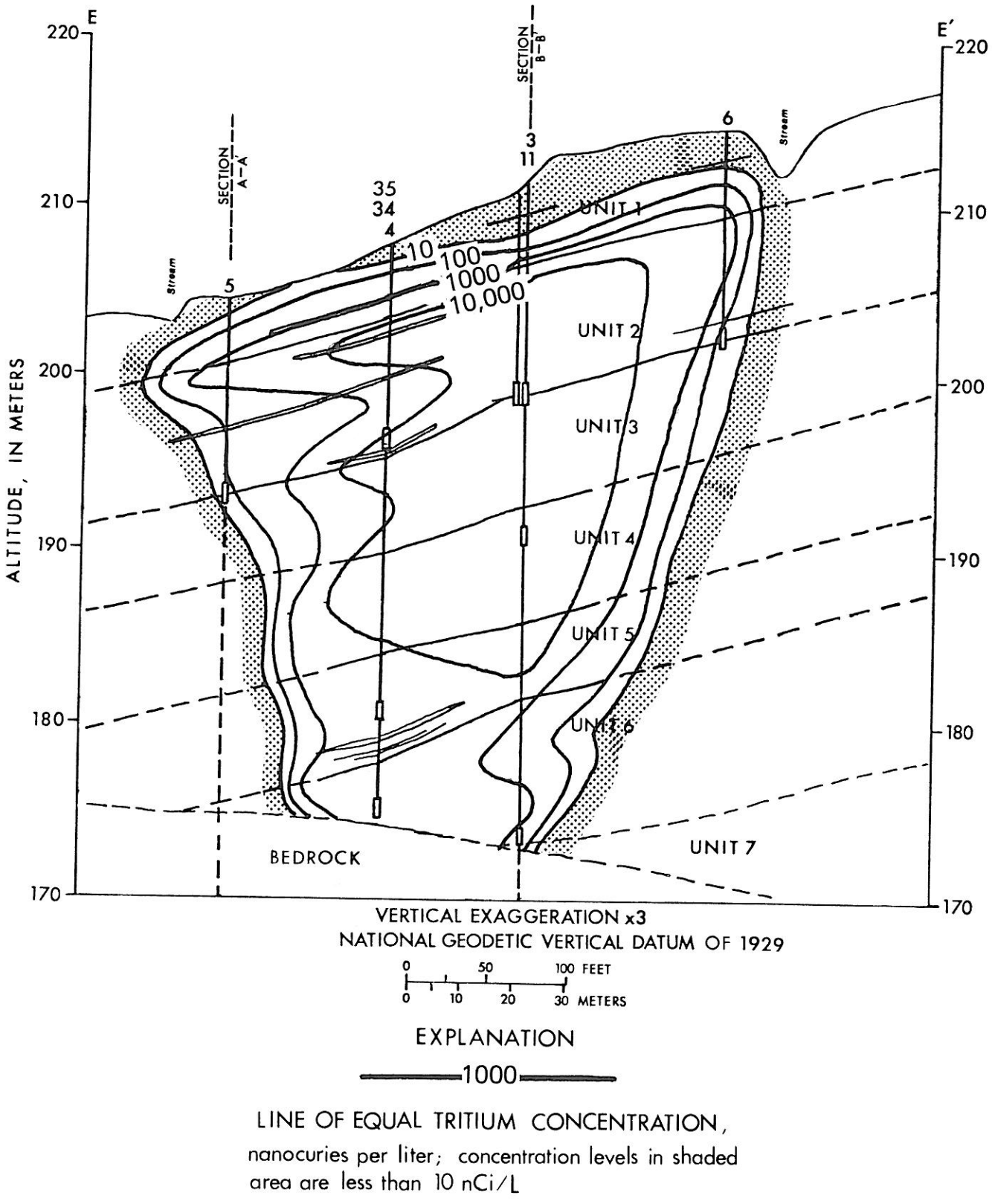

Figure 13. Cross-section *E–E′* through the Plot M site showing the extent of tritium migration and levels of concentration in soil moisture collected from core samples of the drift.

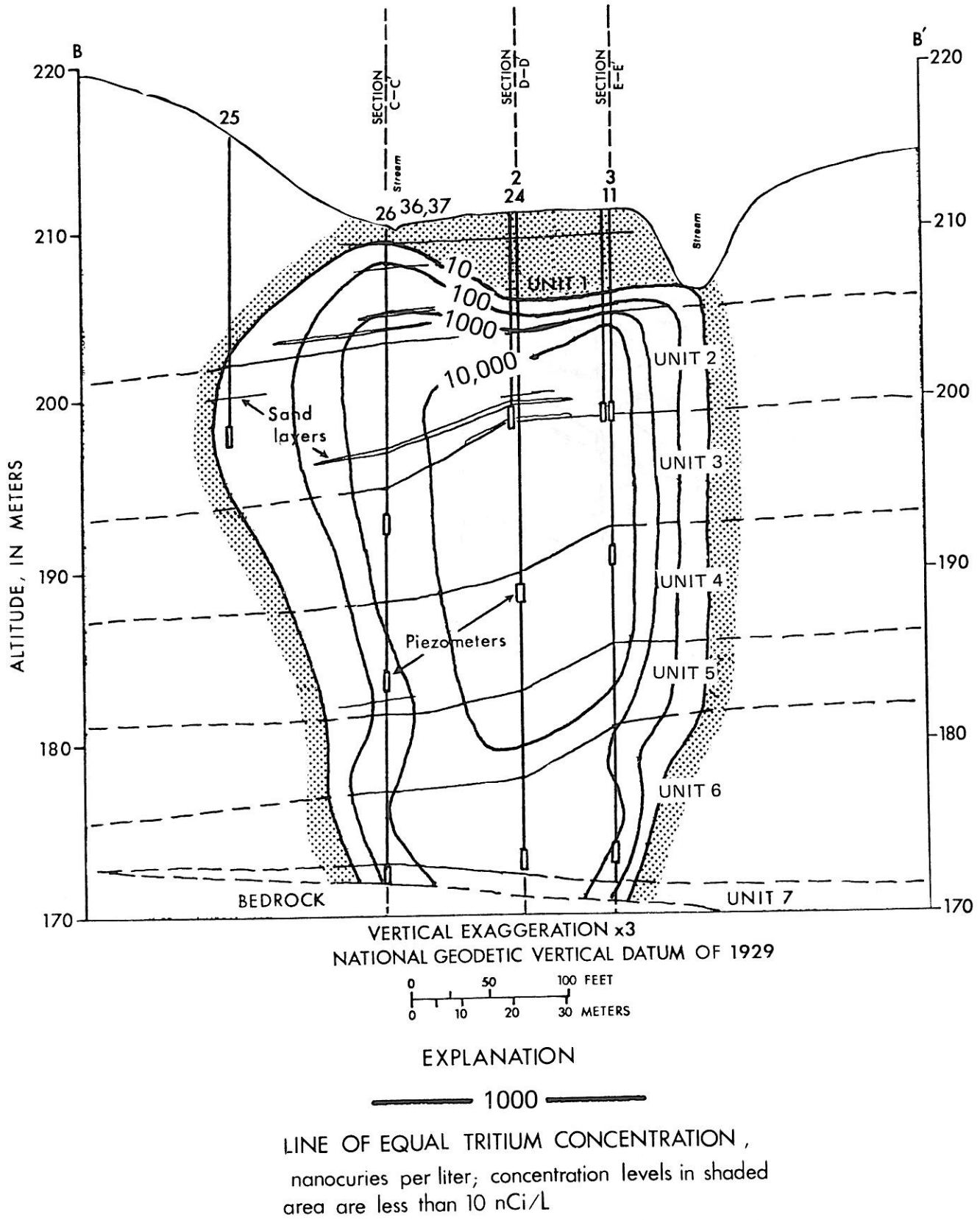

Figure 14. Cross-section *B–B'* on the north side of the Plot M site showing the extent of tritium migration and levels of concentration in soil moisture collected from core samples of the drift.

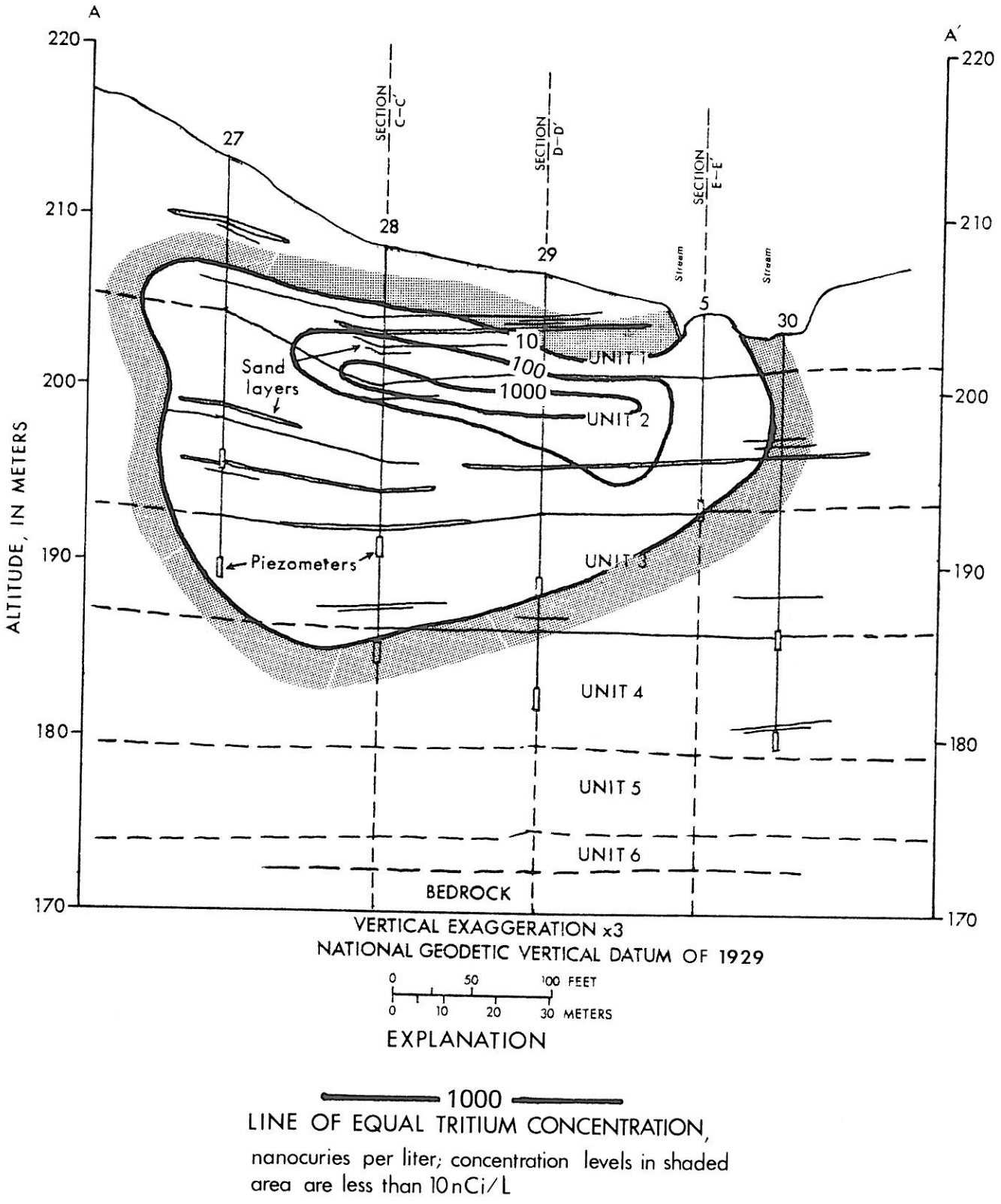

Figure 15. Cross-section *A–A'* 50 m north of the Plot M site showing the extent of tritium migration and levels of concentration in the drift in soil moisture collected from core samples of the drift.

section A–A' is 110 m, which is approximately the same as that in section B–B'. However, the plume is considerably thinner (from top to bottom), and highest tritium concentration levels, exceeding 1,000 nCi/L, are located in a small, thin zone near the surface. This zone underlies numerous sand layers in Unit 1 near test wells 28 and 29. Tritium concentration levels diminish to the east at test well 30 and to the west at test well 27.

The estimated total volume of the tritium plume is 2.56×10^5 m^3, equivalent to a rectangular volume of dimensions 80 m $\times$ 80 m $\times$ 40 m. If the average total porosity of the drift is conservatively estimated to be 30 percent, then the total volume of pore space occupied by tritiated water is 7.68×10^4 m^3.

DISCUSSION

The Single Slug Theory

The evolution of the tritium plume from the mid-1940's to the present is poorly understood owing to the lack of pre-1970 subsurface data. There is no knowledge of the former shape, size, and concentration levels of the plume because core samples were not collected prior to 1976, because there are no data on the rate of tritium migration out of the burial trenches, and because the process that formed the plume is not clearly understood. The following discussion presents a theory of the evolution of the tritium plume based on the evidence gathered during the last 4 years.

Before construction of the concrete cap in 1956, infiltrating water from precipitation leached tritium to the ground-water system. The pattern of tritium concentration in the plume indicates that it is not an accumulation of 13 annual slugs of tritium (1943–56). The single "bull's-eye" pattern suggests that the plume resulted from a single slug—either one large slug due to above-normal recharge in 1 year or a series of slugs that coalesced over a small number of years.

Several facts support the single slug theory:

1. The burial trenches were exposed to precipitation until mid-1956. The concrete cap either stopped the migration of most of the tritium from the trenches or effectively stopped the leaching process.
2. Since 1976, when analyses of water samples from the piezometers began, tritium concentration levels in water in most of the Unit 2 piezometers (1, 2, 4, 5, 6, and 8) have decreased steadily. On the other hand, tritium concentration levels in water from the deepest piezometers in Unit 6 [piezometers 24 (38 m) and 11 (38 m)] have increased. The rate of change of tritium concentration in the uppermost piezometers is greater than the rate of concentration change due to radioactive decay. These data indicate that water with increasingly higher tritium content is entering the piezometers, that is, that the slug is moving downward to deeper levels of the drift.
3. The seasonal fluctuations of tritium concentration levels in water at the Red Gate Woods well are a rough measure of the relative amount of tritium entering the dolomite from the drift. The highest annual tritium concentration levels have been constant over the last 7 years. If these concentration levels are adjusted for radioactive decay since 1973, tritium concentration levels in the water have actually increased slightly. The increase in tritium concentration levels in water at the Red Gate Woods well supports the conclusions (in item 2 above) that the center of the plume is moving deeper into the drift beneath Plot M and that increasingly higher concentration levels of tritium are entering the dolomite.

Tritium Migration Rate

Although this study has determined that the leading edge of the plume, or sharp front (the 10 nCi/L boundary), has moved 40 m downward through the drift to the underlying bedrock surface, the data indicate neither when the front left the burial site nor when it reached the surface. However, the relatively large surface areas of the plume-bedrock contact, the near-vertical lines of equal concentration at the contact, and the elevated levels of tritium in the center of the plume just above the contact, considered together, suggest that the front reached the bedrock surface several years ago. The discovery of tritiated water in the Red Gate Woods well in 1973 sets an arrival time as far back as the early 1970's.

These data yield a limiting value of the bulk vertical rate of tritium migration in the drift. A movement of the front 40 m in the maximum amount of time possible (about 20 years, 1950–70) is equivalent to a rate of 6.3×10^{-6} cm/s. Interestingly, this value is well within the range of hydraulic conductivity values determined by field and laboratory tests.

Factors Favoring Tritium Migration at the Plot M Site

The results of the study show that Plot M is constructed in tight, low-permeability glacial sediments that do not permit fast rates of tritium migration along shortened flow paths. Few factors favor migration at the site; the following factors are related in part to several physical characteristics of the site and in part to the history of the site.

1. Tritium moves as water. Laboratory analyses to determine tritium distribution on sediment samples at the

site (D. Sherwood, written commun., 1981) show that the mobility of tritium is the same as ordinary water. This agrees with many field studies of similar sediments (Ames and Rai, 1978). Thus, tritiated water occupies and flows unrestricted through all pore spaces in the drift.

2. The fractures in the near-surface drift and the inclined sand layers in Units 1 and 2 aid infiltration and cause lateral northward movement of tritiated water. This movement tends to spread contaminated water throughout a larger volume of drift, enlarging the size of the plume.
3. The underlying dolomite bedrock is a significant, although less important, factor favoring migration at the site. The highly permeable bedrock acts as a drain for the ground water in the drift. A large vertical total head gradient at the base of the drift induces downward water movement.
4. Surface water may be channeled into the drift beneath the burial site (and beneath the vertical concrete walls) by the numerous slanting animal burrows in the ravine walls skirting the site and by horizontal ground-water flow.

Factors Limiting Tritium Migration at the Plot M Site

Many factors combine to limit the rate and extent of tritium migration and the amount and concentration level of tritium in the drift. The most important factors are summarized as follows:

1. The limited volume of tritiated waste and the long elapsed period of burial relative to the radioactive half-life of tritium are major limiting factors. Because of the lack of records, it is impossible to determine accurately the amount of tritium buried at Plot M. However, the total volume of buried radioactive waste is small (300 m^3), and the amount of tritiated waste probably represents a much smaller proportion of the total amount. The short period of burial operations and the estimated slow rate of waste accumulation in the burial trenches also limited the amount of tritium buried. Approximately 2 tritium half-lives have elapsed (24.8 years) since the concrete cap was installed. Seventy-five percent of the original amount of tritium has decayed.
2. The drift is thick, dense, and composed chiefly of clay and silt. The hydraulic conductivity of the drift is very low, and intergranular flow predominates. Channelized flow in fractures and in sand lenses and layers is limited to only a few zones in the upper part of the drift.
3. The hydraulic properties of the drift limit the extent of tritium migration. A vertical total head gradient characterizes most of the drift, directing tritium migration downward. The tightness, density, and low total head gradient in Units 4 and 5 act to slow the rate of vertical migration.

SUMMARY AND CONCLUSIONS

Test wells were drilled into the drift at the Plot M site to determine the geologic and hydrologic characteristics of the drift, to install a network of piezometers, to monitor the vertical and horizontal total head gradients within the ground-water system of the drift, and to determine the extent of tritium migration in the drift. Core samples were collected at each test well for determination of geologic, geochemical, and radiological properties. Geophysical logs were run on each well to provide additional qualitative information of the lithology, density, and moisture content of the drift. Four test wells were drilled into the underlying dolomite bedrock to monitor ground-water levels, to collect water samples for radiological analysis, and to conduct preliminary pump and packer testing.

The drift at the site is composed of two till sheets: the surficial Wadsworth Till and the underlying Malden Till. The till sheets are divided into seven lithologic units on the basis of such characteristics as mineralogy, color, density, grain size, and moisture content. With the aid of geophysical logs, Units 1–7 were correlated between boreholes to determine drift stratigraphy and structure.

Units 1–6 range in thickness from 3 to 6 m, and the distribution of sand, silt, and clay varies systematically with depth. Clay content ranges from 35 to 45 percent in Unit 1 sediments to less than 10 percent in Unit 5 sediments. Unit 6 is composed chiefly of silt and sand, and Unit 7 contains mostly sand and gravel.

Vertical total head gradients characterize the saturated zone in the drift; thus the primary direction of ground-water flow is downward. A horizontal gradient in Units 1 and 2, from the south to the north side of the site, reflects northward ground-water movement along the dipping sand layers in those units. Field bailer tests of piezometers and laboratory tests of core samples show that the hydraulic conductivity of the drift ranges from 1.0×10^{-6} to 1.0×10^{-8} cm/s. Laboratory tests further show no significant difference between values of horizontal and vertical hydraulic conductivity, either within one unit or between units.

Radionuclide analyses of moisture extracted from core samples show that tritium has migrated from the burial trenches into the drift. The tritium plume, defined to be the contaminated zone in the drift in which tritium concentration levels exceed 10 nCi/L, has migrated horizontally northward at least 50 m and 40 m vertically downward to the bedrock surface. Tritium concentration levels in core samples collected just above bedrock are higher than 1,000 nCi/L.

The diameter of the plume decreases with depth, and the elongate shape of the plume supports hydrologic data indicating that the tritiated water moves primarily downward in the drift. Several small zones, or lobes, of relatively high tritium concentration protrude northward from the plume. These lobes correspond with horizontal tritium movement along inclined sand layers in Units 1 and 2.

At present, the edge, or front, of the plume (the 10 nCi/L boundary) intersects the underlying bedrock surface. The front moved from Plot M 40 m downward to bedrock in about 20 years, a rate equivalent to 6.3×10^{-6} cm/s. The center of the plume is 15 m beneath the burial site. The size, shape, and "bull's-eye" concentration pattern of the plume indicate that

1. The plume is a single slug that resulted from infiltration of water either during 1 year or during a small number of years.
2. The burial site is no longer releasing tritium into the drift.
3. The plume is moving deeper into the drift, and higher tritium concentration levels are reaching the deepest piezometers and the bedrock surface.
4. The near-vertical pathway of tritium migration extends from the burial site to the bedrock; the data clearly show that tritium does not move horizontally through the drift from Plot M to the Red Gate Woods well.

Fractures and sand layers cause a small amount of near-surface, horizontal tritium migration which enlarges the tritium plume. The small amount of tritium in the burial trenches and in the drift, the age of the tritiated waste, and the large volume of low-permeability sediments beneath Plot M all play an important role in limiting the amount, direction, and rate of tritium migration.

SELECTED REFERENCES

Ames, L. L., and Rai, Dhanpat, 1978, Radionuclide interactions with rock and soil media, Volume I: Processes influencing radionuclide mobility and retention; Element chemistry and geochemistry; Conclusions and evaluation: U.S. Environmental Protection Agency, 520/6–78–007, 295 p.

Bloyd, R. M., Jr., 1975, Summary appraisals of the nation's ground-water resources—Upper Mississippi Region: U.S. Geological Survey Professional Paper 813–B, 22 p.

Golchert, N. W., and Sedlet, Jacob, 1978, Radiological survey of Site A and Plot M: U.S. Department of Energy Report DOE/EV–0005/7, 89 p.

Golchert, N. W., Sedlet, Jacob, and Hayes, K. A., 1983, Environmental surveillance of the Palos Park Forest Preserve: U.S. Department of Energy Report ANL–83–6, 67 p.

Grisak, G. E., and Jackson, R. E., 1978, An appraisal of the hydrogeological processes involved in shallow subsurface radioactive waste management in Canadian terrain: Ottawa, Canada, Inland Water Directorate, Water Resources Branch, Scientific Series No. 84, 193 p.

Horbert, Leland, and Potter, P. F., 1955, Stratigraphic and sedimentologic aspects of the Lemont Drift of northeastern Illinois: Illinois State Geological Survey Report of Investigation 185, 23 p.

Lineback, J. A., 1979, Quaternary deposits of Illinois: Illinois State Geological Survey Map.

Matthai, H. F., 1979, Hydrologic and human aspects of the 1976–1977 drought: U.S. Geological Survey Professional Paper 1130, 84 p.

Olimpio, J. C., 1980, Low-level radioactive-waste burial at the Palos Forest Preserve, Illinois, Part I. Preliminary finite-difference models of steady state ground-water flow: U.S. Geological Survey Open-File Report 80–775, 40 p.

———1982, Data for wells at the low-level radioactive-waste burial site in the Palos Forest Preserve, Illinois: U.S. Geological Survey Open-File Report 82–692, 99 p.

U.S. Environmental Protection Agency, 1973, Water quality criteria, 1972: EPA–R3.–73.033, Washington, D.C., U.S. Government Printing Office, 594 p.

Willman, H. B., 1971, Summary of the geology of the Chicago area: Illinois State Geological Survey Circular 460, 77 p.

Willman, H. B., and Frye, J. C., 1970, Pleistocene stratigraphy of Illinois: Illinois State Geological Survey Bulletin 94, 204 p.

Willman, H. B., Glass, H. D., and Frye, J. C., 1963, Mineralogy of glacial tills and their weathering profiles in Illinois. Part 1—Glacial tills: Illinois State Geological Survey Circular 347, 55 p.